

# Transcriptomic responses in the nervous system and correlated behavioural changes of a cephalopod exposed to ocean acidification

Jodi Thomas<sup>1,2</sup>, Roger Huerlimann<sup>2</sup>, Celia Schunter<sup>3</sup>, Sue-Ann Watson<sup>4,5</sup>, Philip Munday<sup>1</sup>, and Timothy Ravasi<sup>2</sup>

<sup>1</sup>Australian Research Council Centre of Excellence for Coral Reef Studies, James Cook University, Townsville, Queensland 4811, Australia

<sup>2</sup>Marine Climate Change Unit, Okinawa Institute of Science and Technology Graduate University, Okinawa, Japan

<sup>3</sup>Swire Institute of Marine Science, School of Biological Sciences, The University of Hong Kong, Pok Fu Lam, Hong Kong SAR

<sup>4</sup>College of Science and Engineering, James Cook University, Townsville, Queensland 4811, Australia

<sup>5</sup>Biodiversity and Geosciences Program, Museum of Tropical Queensland, Queensland Museum Network, Townsville, Queensland 4810, Australia

July 31, 2023

## Abstract

The nervous system is central to coordinating behavioural responses to environmental change, likely including ocean acidification (OA). However, a clear understanding of neurobiological responses to OA is lacking, especially for marine invertebrates. We evaluated the transcriptomic response of the central nervous system (CNS) and eyes of the two-toned pygmy squid (*Idiosepius pygmaeus*) to OA conditions, using a *de novo* transcriptome assembly created with long read PacBio ISO-sequencing data. We then correlated patterns of gene expression with CO<sub>2</sub> treatment levels and OA-affected behaviours in the same individuals. OA induced transcriptomic responses within the nervous system related to various different types of neurotransmission, neuroplasticity, immune function and oxidative stress. These molecular changes may contribute to OA-induced behavioural changes, as suggested by correlations between gene expression profiles, CO<sub>2</sub> treatment and OA-affected behaviours. This study provides the first molecular insights into the neurobiological effects of OA on a cephalopod and correlates molecular changes with whole animal behavioural responses, helping to bridge the gap in our knowledge between environmental change and animal responses.

## 1. Introduction

As human-induced environmental changes progress, establishing how animals respond to projected future environmental conditions, and why these responses occur, is critical (Fuller *et al.*, 2010). A thorough understanding of why biological responses are occurring is especially useful for gaining insight into why some individuals or species are more sensitive to environmental change than others, and improving predictions of how organisms and populations will respond over the time scales at which environmental change is occurring (Cooke *et al.*, 2013). The nervous system forms the fundamental link between the environment and an animal's responses (Kelley *et al.*, 2018; O'Donnell, 2018). Thus, the neurobiological impacts of anthropogenic environmental change are key to understanding how animals will respond as environmental change

progresses, yet the role of the nervous system in biological responses to environmental change has been little explored (Kelley *et al.*, 2018).

The uptake of anthropogenic carbon dioxide (CO<sub>2</sub>) by the ocean is causing seawater CO<sub>2</sub> levels to rise, decreasing seawater pH and altering the concentration of carbonate ions, in a process known as ocean acidification (OA) (Bindoff *et al.*, 2019). These chemical changes can fundamentally affect marine organisms and the ecosystems they inhabit (Doney *et al.*, 2009). OA affects a wide variety of physiological processes, life history traits and behaviours of marine invertebrates (Durant *et al.*, 2023; Kroeker *et al.*, 2010; Nagelkerken & Connell, 2015; Pörtner *et al.*, 2004; Thomas *et al.*, 2020). Invertebrates are vital components of marine ecosystems, comprising over 92% of species in the ocean, are essential to the function of ecosystem processes, and support the livelihoods of human societies across the globe (Bertness *et al.*, 2001; Chen, 2021). Animal behaviour influences an individual's own fitness, complex interactions with other individuals and species, and key ecological processes that shape the structure of marine communities and ecosystems (Nagelkerken & Munday, 2015). Consequently, any behavioural effects of elevated CO<sub>2</sub> on marine invertebrates could potentially have wide-ranging ecological, social and economic consequences.

Despite many studies assessing the behavioural responses of marine invertebrates to OA the link between the environment and behavioural responses, the nervous system, has been largely understudied. The work that has addressed the neurobiological impacts of OA has focused on the functioning of GABA<sub>A</sub> receptors. The GABA hypothesis was first proposed in fish and suggests acid-base regulatory mechanisms occurring at elevated CO<sub>2</sub> conditions alter ionic gradients across neuronal membranes, consequently disturbing GABA<sub>A</sub> receptor function and causing behavioural alterations (Nilsson *et al.*, 2012). A range of research has supported the GABA hypothesis in fish (reviewed in Heuer *et al.* (2019)), and more recently pharmacological studies have also supported the GABA hypothesis in molluscs (Clements *et al.*, 2017; Thomas *et al.*, 2021; Watson *et al.*, 2014), but not a crustacean (Charpentier & Cohen, 2016). However, OA may also have a range of other neurobiological impacts, including altering the function of other ligand-gated ion channels that are similar to the GABA<sub>A</sub> receptor (Thomas *et al.*, 2021) and affecting synaptic plasticity (Lai *et al.*, 2017; Porteus *et al.*, 2018).

Transcriptomics provides a powerful non-targeted, holistic approach to identify functional responses to environmental change. Indeed, transcriptomics has widely been taken up by the OA research community to understand the response of marine animals to elevated CO<sub>2</sub> (Strader *et al.*, 2020). However, there is less research assessing the transcriptomic response of nervous tissue to elevated CO<sub>2</sub>. Recently, studies have examined the transcriptomic response of the fish nervous system to elevated CO<sub>2</sub> conditions, including in coral reef fishes (Kang *et al.*, 2022; Schunter *et al.*, 2021; Schunter *et al.*, 2019; Schunter *et al.*, 2018; Schunter *et al.*, 2016), temperate marine fishes (Cohen-Rengifo *et al.*, 2022; Porteus *et al.*, 2018; Toy *et al.*, 2022) and ocean-phase salmon (Williams *et al.*, 2019). In marine invertebrates, two transcriptomic studies assessing the whole-body response of pteropod molluscs to elevated CO<sub>2</sub> identified altered expression of genes involved in nervous system function (Johnson & Hofmann, 2017; Moya *et al.*, 2016). However, whole body measurements cannot determine if non-tissue-specific transcripts are responding to elevated CO<sub>2</sub> in a system-wide manner, or only within specific tissues. Furthermore, due to the heterogeneity and complexity of gene expression, measurements at the whole-body level may mask transcriptomic responses in specific tissues, such as the nervous system.

Here, we investigated the transcriptomic response to OA in the central and peripheral nervous system of a cephalopod, the two-toned pygmy squid (*Idiosepius pygmaeus*), and then correlated the molecular responses with behavioural changes recorded in the same individuals. Cephalopods have complex nervous systems and behaviours rivalling those of fishes (Hanlon & Messenger, 2018), making them a useful taxon to investigate the neurobiological impacts of elevated CO<sub>2</sub>. *I. pygmaeus* is a diurnal, tropical squid inhabiting shallow, inshore waters of the Indo-Pacific, including Northern and North-eastern Australia (Moynihan, 1983; Reid, 2005). They are a small, short-lived squid growing to a maximum mantle length of 2 cm (Reid, 2005), and have a lifespan of up to 80 days (Jackson, 1988). *I. pygmaeus* is an ideal species to use as previous research in this species found elevated CO<sub>2</sub> alters a range of behaviours (Spady *et al.*, 2018; Spady *et al.*, 2014; Thomas

*et al.*, 2021).

In this study, we used RNA from the central nervous system (CNS) and eyes (peripheral sense organ) from squid exposed to current-day ( $\sim 400 \mu\text{atm}$ ) or elevated ( $\sim 1,000 \mu\text{atm}$ )  $\text{CO}_2$  levels for 7 days in a previous study by Thomas *et al.* (2021). In these squid, elevated  $\text{CO}_2$  exposure increased activity levels as well as visually-guided, conspecific-directed attraction and aggression (Thomas *et al.*, 2021). Here, we created a *de novo* transcriptome assembly, providing a reference which we used to determine the transcriptomic response of the squid CNS and eyes to elevated  $\text{CO}_2$ . We used the eyes because cephalopods, including squid, are highly visual animals with many visually-guided behaviours (Chung *et al.*, 2022; Mather, 2006; Muntz, 1999). Furthermore, we have shown elevated  $\text{CO}_2$ -induced disturbances of visually-guided behaviour in the same squid used in this study (Thomas *et al.*, 2021). As we had transcriptomic and behavioural data from the same individual squid, we also correlated patterns of gene expression with  $\text{CO}_2$  treatment levels and OA-affected behaviours to determine key genes and processes in the cephalopod CNS and eyes potentially contributing to OA-induced behavioural changes. The results from this study help us understand, at a molecular level, the neurobiological impacts of ocean acidification in a marine invertebrate with a complex nervous system.

## 2. Methods

### 2.1 Animal collection and experimental setup

The squid tissues and behavioural data used in this study came from a previous experiment. Specifically, we used sham-treated squid from the picrotoxin experiment in Thomas *et al.* (2021) (Figure 1). As described in Thomas *et al.* (2021), male two-toned pygmy squid (*Idiosepius pygmaeus*) were collected from the wild and acclimated in groups at current-day seawater conditions for 1 - 6 days before transferral to individual treatment tanks set at either current-day ( $\sim 400 \mu\text{atm}$ ) or elevated ( $\sim 1,000 \mu\text{atm}$ )  $\text{CO}_2$  levels, consistent with  $\text{CO}_2$  levels projected for 2100 following the representative concentration pathway RCP8.5 scenario (Bindoff *et al.*, 2019). Experiments were carried out in four interconnected 8,000 L recirculating seawater systems; two untreated seawater systems were used for current-day  $\text{CO}_2$  treatments, and two seawater systems were dosed with  $\text{CO}_2$  using a custom-built pH control system for elevated  $\text{CO}_2$  treatments. The  $\text{CO}_2$  conditions achieved were current-day  $\text{CO}_2$ :  $407 \pm 58 \mu\text{atm } p\text{CO}_2$ ,  $\text{pH}_T = 8.09 \pm 0.10$  and elevated  $\text{CO}_2$ :  $1,071 \pm 71 \mu\text{atm } p\text{CO}_2$ ,  $\text{pH}_T = 7.73 \pm 0.03$  (mean  $\pm$  SD). Refer to Thomas *et al.* (2021) for further details.  $\text{CO}_2$  variation is common in coastal habitats (Hannan *et al.*, 2020). However, the coastal waters where we collected *I. pygmaeus* show little daily variation in seawater  $p\text{CO}_2$  levels; average daily range  $20.3 \pm 8.6 \mu\text{atm } \text{CO}_2$  (mean  $\pm$  SD) (Supplementary Text S1 and Figure S1). Thus, our experimental  $\text{CO}_2$  levels are ecologically relevant to the population of *I. pygmaeus* used.

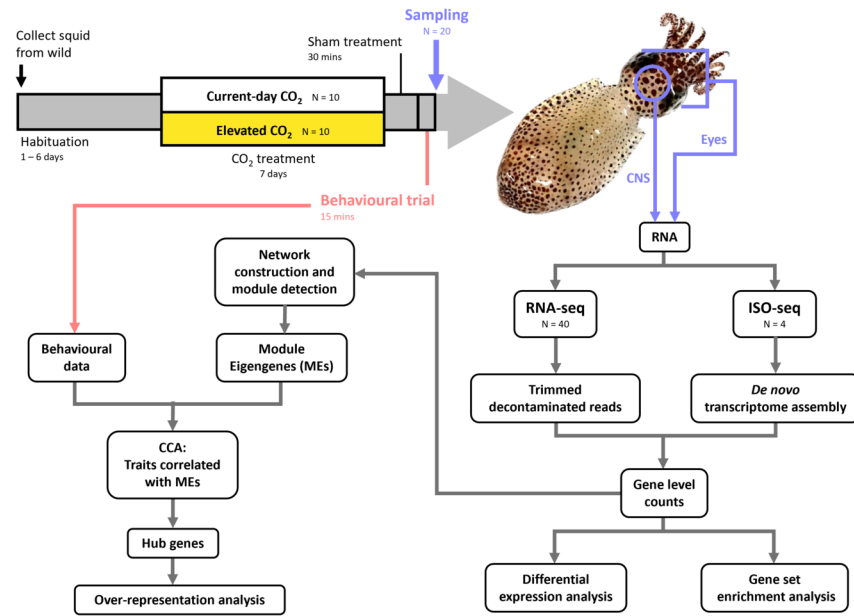


Figure 1: **Experimental design overview.** CCA = canonical correlation analysis. *Idiosepius pygmaeus* photograph by Jodi Thomas.

## 2.2 Behavioural analysis

After 7 days of current-day or elevated CO<sub>2</sub> treatment, squid underwent sham treatment by being individually placed in 100 mL of aerated seawater from their CO<sub>2</sub> treatment containing 0.2% ethanol for 30 minutes, as part of the experiment by Thomas *et al.* (2021). Visually-guided behaviour was then tested for 15 minutes by placing squid individually in a tank (30×30×15 cm) filled to 3 cm depth with seawater from their CO<sub>2</sub> treatment and with a mirror taking up the entire area of one wall. Three aspects of squid behaviour shown to be altered by elevated CO<sub>2</sub> in Thomas *et al.* (2021), activity level, aggressive conspecific-directed behaviour and exploratory conspecific-directed behaviour (Table 1), were used here. See Thomas *et al.* (2021) for a detailed description of the behavioural analysis and results.

## 2.3 Tissue sample collection

Immediately after each behavioural trial, squid were euthanised with AQUI-S (1:1000). The head was separated from the mantle, rinsed in distilled water, and blotted dry. The skin, tentacles, beak, and buccal mass were removed and the eyes and central nervous system (CNS, containing the oesophagus running through the middle) were dissected and snap frozen in liquid nitrogen within  $4.18 \pm 0.55$  (mean  $\pm$  SD) minutes after euthanasia. Tissues were then transferred to -80°C for storage. This study followed the animal ethics guidelines at James Cook University (JCU animal ethics number A2644).

## 2.4 RNA extraction

Total RNA was extracted from the entire CNS, and both eyes combined for each squid ( $n_{\text{current-day CO}_2} = 10$ ,  $n_{\text{elevated CO}_2} = 10$  for each tissue) (Figure 1). Each tissue sample was homogenised in RLT-Plus Buffer (Qiagen) with sterile zirconia/silica beads (1mm diameter, BioSpec Products) in a Mini-BeadBeater 96 (BioSpec Products) for a total of 2 minutes. Total RNA was extracted using an AllPrep DNA/RNA Mini Kit (Qiagen). RNA integrity of all 40 samples was measured on an Agilent 2200 TapeStation (High Sensitivity RNA ScreenTape, Agilent) (Supplementary File S1).

## 2.5 RNA sequencing

The Sequencing Section, Okinawa Institute of Science and Technology Graduate University, Japan carried out library preparation and sequencing on all 40 RNA samples. RNA was quantified by Qubit Flex Fluorometer (Qubit RNA BR assay kit, Thermo Fisher Scientific Inc.). The NEBNext® Poly(A) mRNA Magnetic Isolation Module (New England BioLabs Inc.) was followed according to the manufacturers protocol to isolate mRNA. One library was prepared for each sample, using the NEBNext® Ultra II Directional RNA Library Prep Kit for Illumina® (New England BioLabs Inc.) following the manufacturers protocol, using ten PCR cycles. Libraries were sequenced on two lanes of a NovaSeq6000 with a S2 flow cell paired end to the length of 150 bp.

## 2.6 RNA-seq read pre-processing

For a detailed workflow of the bioinformatic and statistical analyses, see Supplementary Figure S2. Raw reads were inspected with FastQC (v0.11.9) (Andrews, 2010) and MultiQC (v1.9) (Ewels *et al.*, 2016) and trimmed with Fastp (v0.21.1) (Chen *et al.*, 2018) using a sliding window of 4 bp, a mean Phred score of 30 and reads < 30 bp were trimmed. Kraken2 (v2.0.9) (Wood *et al.*, 2019) was used with a confidence of 0.3 to remove any contamination using the NCBI bacterial and archaeal reference libraries (downloaded 08/2020).

## 2.7 Read mapping and counting

As a reference for gene expression quantification, we created and annotated a *de novo* transcriptome assembly of *I. pygmaeus* CNS and eye tissues using long read PacBio ISO-sequencing data. Refer to Supplementary Text S2 for a description of the methods for ISO-sequencing, *de novo* transcriptome assembly, and transcriptome annotation. The trimmed and decontaminated RNA-seq reads were mapped against the transcriptome assembly using salmon (v1.3.0) (Patro *et al.*, 2017). Correction for sequence-specific biases and fragment-level GC biases was used, the quantification step was skipped, and the flags ‘-validateMappings’ and ‘-hardFilter’ were also used. Corset (v1.09) (Davidson & Oshlack, 2014) was run on the salmon equivalence class files from all 40 samples to cluster the transcripts to gene-level and produce gene-level counts. In Corset, we provided the four groups/treatments (eyes current-day CO<sub>2</sub>, eyes elevated CO<sub>2</sub>, CNS current-day CO<sub>2</sub> and CNS elevated CO<sub>2</sub>), the log likelihood ratio test was switched off to prevent differentially expressed transcripts being split into different clusters, and the links between contigs were removed if the link was supported by less than 10 reads.

## 2.8 Statistical analyses

All statistical analyses (as described below) were carried out in R (v4.0.4) (R Core Team, 2021), primarily using RStudio (v 1.4.1106) (RStudio Team, 2021).

### 2.8.1 Differential expression analysis

DESeq2 (v1.30.1) (Love *et al.*, 2014) using the Wald test was used to compare gene expression between current-day and elevated CO<sub>2</sub> conditions for the CNS and eyes separately. Genes with an adjusted p-value (padj, Benjamini-Hochberg method) < 0.05 were reported as differentially expressed (DE). Log2fold change estimates were shrunk with the ashR method (Stephens, 2016) to increase their accuracy.

### 2.8.2 Gene set enrichment analysis

Gene set enrichment analysis (GSEA) was run in clusterProfiler (v3.18.1) (Yu *et al.*, 2012) for each tissue separately to determine if sets of genes from the same gene ontology (GO) term/functional category showed significant, concordant differences between current-day and elevated CO<sub>2</sub> conditions. Unweighted GSEA was run using the DESeq2 log2 fold-change values of all genes and the annotated GO terms as the ‘gene sets’. A minimum and maximum gene set size of 15 and 500, respectively, was used. GSEA determines if genes from the same functional category are significantly more likely to occur at the top or bottom of the log2 fold-change list and therefore whether these functional categories are up- or down-regulated at elevated CO<sub>2</sub>, respectively. P-values were adjusted for multiple comparisons using the Benjamini-Hochberg method and a significance threshold of padj < 0.05 was used. The GSEA results were imported into Cytoscape (v3.8.2)

(Shannon *et al.*, 2003) where EnrichmentMap (v3.3.1) (Merico *et al.*, 2010) was used to create a network to visualise the functional enrichment results. All significant functional categories were included in the network as a circular node. Functional categories with  $> 0.25$  similarity were linked by edges. Similar functional categories were manually grouped into clusters and labelled.

### 2.8.3 Correlating gene expression profiles with CO<sub>2</sub> treatment and OA-affected behaviours

To analyse the correlation between gene expression and behavioural traits of squid across CO<sub>2</sub> treatments, we employed weighted gene co-expression network analysis (WGCNA) followed by canonical correlation analysis (CCA) on the CNS and eyes, separately (Figure 1). Refer to Supplementary Text S3 for a detailed description of the methods for gene co-expression network construction and module detection, module eigengene correlation with behavioural traits, module membership vs gene significance, and identification of hub genes (Figures S3 – S21, Tables S1 and S2). Briefly, the gene-level counts from DESeq2 (v1.30.1) (Love *et al.*, 2014) were used in the WGCNA package (v1.70-3) (Langfelder & Horvath, 2008) to construct a co-expression network and detect modules of genes. A module eigengene was calculated for each module of genes, representing the gene expression profiles of that module. CCA using package CCA (v1.2.1) (González *et al.*, 2008) was used to explore the correlations between the two sets of variables from the same individual squid: ME set = module eigengenes from each module; traits set = CO<sub>2</sub> level (current-day or elevated) and behavioural traits (active time (s), distance (cm), speed (cm/s), time in Zone A (s), whether the squid displayed an exploratory/aggressive interaction (yes/no), number of exploratory/aggressive interactions). For those modules identified by CCA to be correlated with each trait, the Pearson correlation of module membership (MM, higher value indicates the gene is more highly connected to the given module) and gene significance (GS, higher value indicates a more biologically relevant gene) was calculated (Langfelder & Horvath, 2008). A correlation of GS and MM imply that genes more highly connected with a given module also tend to be more highly correlated with the given trait, providing another measure for the importance of this module with the given trait (Langfelder & Horvath, 2008). This identified the final modules of interest, within which the MM and GS values of each gene were used as a screening method to identify biologically relevant, highly interconnected hub genes (Fuller *et al.*, 2007; Horvath & Dong, 2008; Langfelder & Horvath, 2008), i.e. to find genes correlated with CO<sub>2</sub> treatment and each behavioural trait. Hub genes were defined as those genes within the final modules of interest with a very strong correlation with the module (MM  $> 0.8$ ) and a moderate correlation with the given trait (GS  $> 0.4$ ).

All hub genes for CO<sub>2</sub> treatment were compared across tissues to identify hub genes for CO<sub>2</sub> treatment that are CNS-specific, eyes-specific or found in both tissues. Hub genes for CO<sub>2</sub> treatment that were also a hub gene for one or more behavioural traits were identified as genes correlated with the associated OA-induced behavioural change. Finally, functional enrichment analysis was used for the CNS-specific CO<sub>2</sub> treatment hub genes that were also hub genes for all three activity traits in the CNS using over-representation analysis (ORA) in clusterProfiler (v3.18.1) (Yu *et al.*, 2012) with the hypergeometric test. This determined if any GO terms were significantly over-represented within the list of hub genes. All other groups of CO<sub>2</sub> treatment hub genes had 25 or fewer genes and thus ORA was not used. P-values were adjusted for multiple comparisons using the Benjamini-Hochberg method and a significance threshold of  $\text{padj} < 0.05$  was used.

## 3. Results

### 3.1 Transcriptome assembly and annotation

The *de novo* transcriptome assembly for *Idiosepius pygmaeus* was created from a total of 138.6 million PacBio ISO-sequencing subreads and resulted in 49,981 transcripts that were clustered into 27,420 genes. The transcriptome assembly had an N50 of 3,163 bp, 70.4% complete BUSCOs and an  $82.1 \pm 5.5\%$  overall alignment rate of the RNA-seq reads (Table S3). A total of 69% of the transcripts received a functional annotation (Supplementary Table S4). The species distribution of the top blast hits was dominated by cephalopod species (Figure S22). Final mapping of RNA-seq reads against the transcriptome assembly had a  $73.6 \pm 6.9\%$  mapping rate (Table S5).

### 3.2 Differentially expressed genes

We compared gene expression between current-day and elevated CO<sub>2</sub> conditions for the CNS and eyes separately. There was more variance in the eyes than the CNS (Figure 2A). In the CNS, we identified 25 differentially expressed genes (DEGs) between current-day and elevated CO<sub>2</sub> conditions; 14 upregulated and 11 downregulated with elevated CO<sub>2</sub>. In the eyes, there were eight DEGs; five upregulated and three downregulated at elevated, compared to current-day, CO<sub>2</sub> conditions (Figure 2B). Two genes were significantly upregulated with elevated CO<sub>2</sub> in both the CNS and eyes; one essential for autophagy (*ykt6*) and another poorly characterised gene (*fam204a*). In both tissues, the DEGs play roles in neurotransmission (CNS: *folh1*, *syvn1-b*, *slc2a13*, *celsr3*, eyes: *maoa*, *slc18a1*, *cbs*), immune function (CNS: *psenen*, *syvn1-b*, *map4k5*, *tf*, *nme6*, *map1l3ca/b*, eyes: *pglyrp2*, *cbs*, *maoa*), the oxidative stress response (CNS: *tf*, *cyb561d2*, *syvn1-b*, *chrac1*, *ykt6*, eyes: *cbs*, *ykt6*), and transcription regulation (CNS: *nme6*, *chrac1*, *znf271*, eyes: *gtf2e2*) (Table S6).

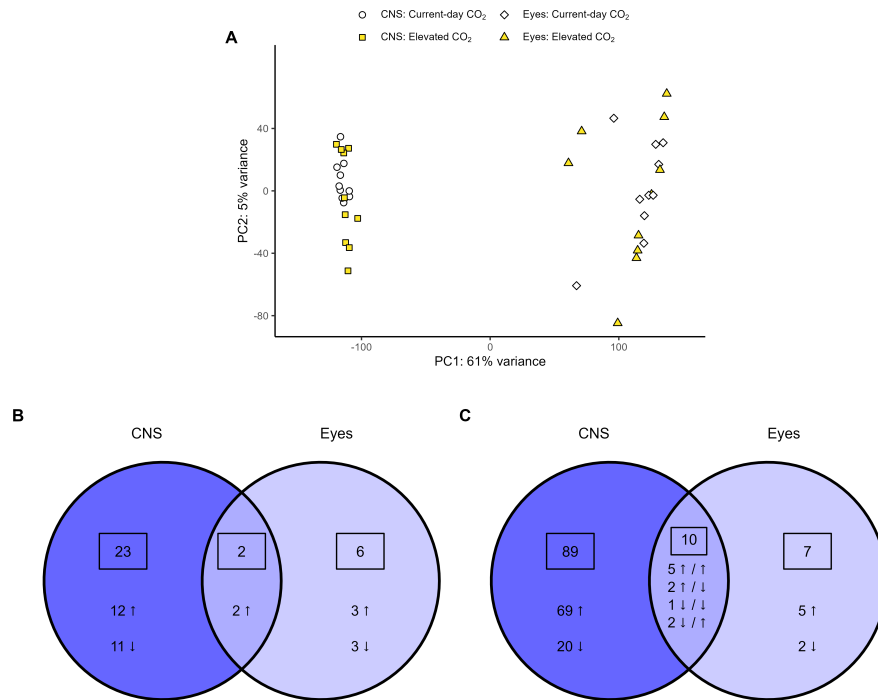


Figure 2: **Differential expression and GSEA results.** **A** PC1 and PC2 axes from the principal components analysis of all genes for the 40 samples. **B** Venn diagram comparing the DEGs between current-day and elevated CO<sub>2</sub> levels in the CNS and eyes. **C** Venn diagram comparing the GO terms / functional categories found to be significantly different between current-day and elevated CO<sub>2</sub> levels in the CNS and eyes by GSEA. circle = CNS current-day, square = CNS elevated CO<sub>2</sub>, diamond = Eyes current-day, triangle = Eyes elevated CO<sub>2</sub>, — = upregulated at elevated CO<sub>2</sub> conditions, — = downregulated at elevated CO<sub>2</sub> conditions.

### 3.3 Small, coordinated changes in expression of genes belonging to the same functional categories

Gene set enrichment analysis (GSEA) identified Gene Ontology (GO) terms/functional categories, across all three GO categories (biological process, molecular function, and cellular component), that were significantly affected by CO<sub>2</sub> treatment, indicating small, coordinated changes in expression of the genes belonging to each of these functional categories. We identified ninety-nine significant functional categories in the CNS; 75 upregulated and 24 downregulated at elevated CO<sub>2</sub> (Figure 2C). These functional categories included those involved in transcription, RNA processing, translation, protein processing, the cell cycle and cell

proliferation, and neurotransmission (Figures 3 and S23). There were 17 significant functional categories in the eyes; 12 upregulated and 5 downregulated at elevated CO<sub>2</sub> (Figure 2C). Ten functional categories were significantly affected by CO<sub>2</sub> treatment in both the CNS and eyes including functions related to the ribosome and translation, ion channels, kinase activity, protein degradation and cell adhesion (Figures 3 and S23).

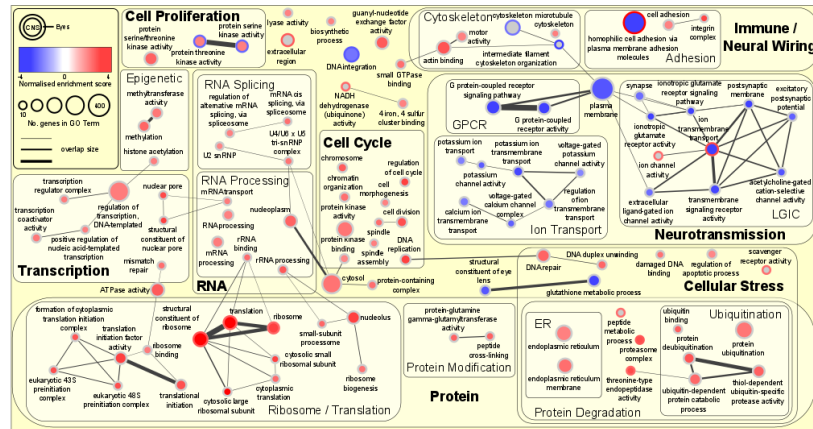


Figure 3: **Enrichment map displaying the gene set enrichment analysis (GSEA) results in both the CNS and eyes.** Significant GO terms/functional categories are represented by a circular node. Results from the CNS and eyes are represented by colouration of the inner node area and node border, respectively. Red represents functional categories upregulated at elevated CO<sub>2</sub> and blue represents functional categories downregulated at elevated CO<sub>2</sub>. Colour intensity represents the normalised enrichment score and node size the number of core enrichment genes in each functional category.

### 3.4 Genes correlated with OA-induced behavioural change

We identified 230 and 25 hub genes for CO<sub>2</sub> treatment in the CNS and eyes, respectively, with 14 CO<sub>2</sub> treatment hub genes shared by both tissues. Of these CO<sub>2</sub> treatment hub genes in the CNS, eyes and both tissues, 169, 6 and 10 genes were also identified as hub genes for one or more behavioural traits, respectively, indicating these genes as potentially correlated with CO<sub>2</sub>-induced behavioural changes (Figure 4). Of the 169 genes in the CNS potentially contributing to CO<sub>2</sub>-induced behavioural changes, 87 were positively correlated with CO<sub>2</sub> treatment and all three activity traits and were significantly enriched for 13 functional categories, including those playing a role in the cell cycle, cell migration, and protein synthesis and folding (Figure 5). Four of these functional categories were also identified as significantly upregulated at elevated CO<sub>2</sub> in the CNS by GSEA; ‘nuclear pore’, ‘motor activity’, ‘chromosome’ and ‘protein kinase binding’. The six transcripts in the eyes potentially contributing to CO<sub>2</sub>-induced behavioural changes had a match for two known genes; an acetylcholine receptor subunit (*chrna10*) and a gene essential for maintaining retinal tissue integrity (*crb*). The 10 transcripts in both tissues potentially contributing to CO<sub>2</sub>-induced behavioural changes had a match for eight known genes, again including *chrna10*, and genes with putative roles in cell proliferation (*gid-4*, *cdk10*) and protein processing (*spr72*, *vhl*, *zranb1*). See Table S7 – S10 for all hub genes identified by WGCNA and their putative functions.

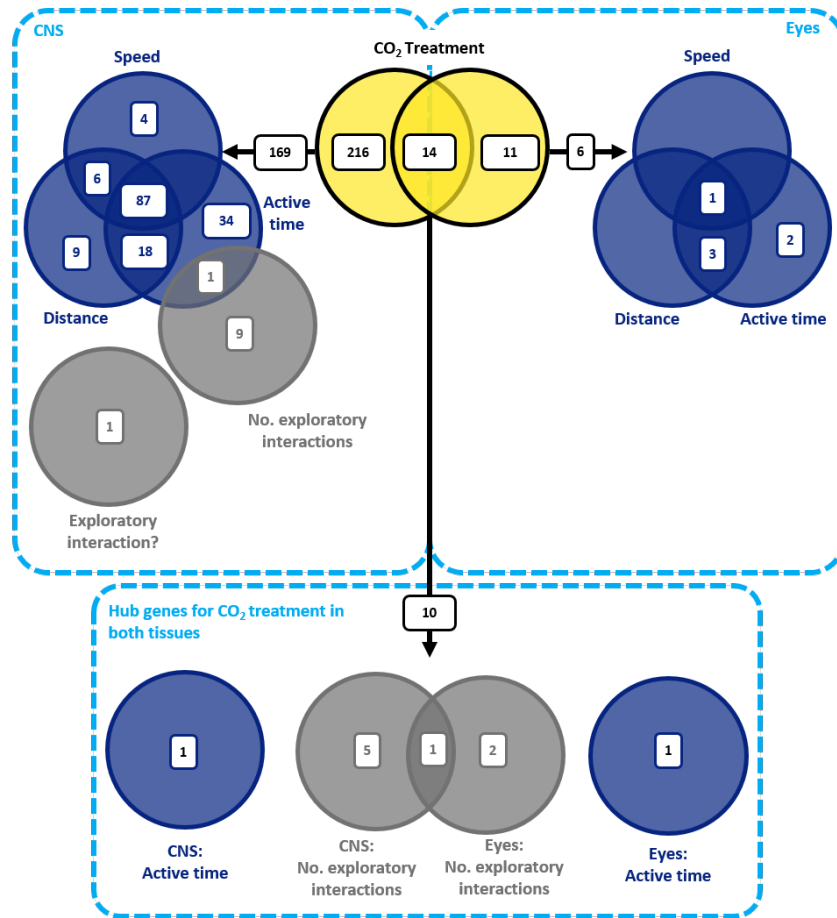


Figure 4: Venn diagram depicting the number of hub genes identified for CO<sub>2</sub> treatment and behavioural traits in the CNS and eyes. The yellow Venn diagram in the centre depicts the number of hub genes for CO<sub>2</sub> treatment that are CNS-specific (left) and eyes-specific (right), and the overlap represents the number of CO<sub>2</sub> treatment hub genes shared by both tissues. CNS-specific and eyes-specific CO<sub>2</sub> treatment hub genes also identified as a hub gene for one or more behavioural traits in the CNS or eyes are on the left and right, respectively. Hub genes for CO<sub>2</sub> treatment found in both tissues, that are also a hub gene for a behavioural trait in one or both tissues, are shown at the bottom centre. CO<sub>2</sub> treatment hub genes shared with activity traits (active time, distance and speed) and exploratory conspecific-directed behaviours (number of exploratory interactions and whether any exploratory interactions occurred) are in blue and grey, respectively. Exploratory interaction? = whether any exploratory interactions occurred (yes/no).

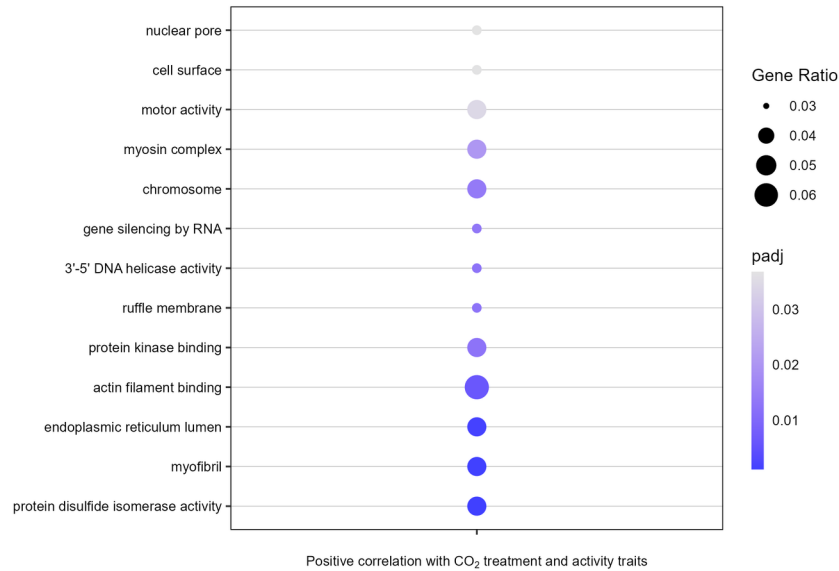


Figure 5: **GO Terms/functional categories significantly enriched from the 87 genes positively correlated with CO<sub>2</sub> treatment and all three activity traits in the CNS.** padj = adjusted p-value, blue indicates higher significance. Gene Ratio = the number of genes represented in the genes positively correlated with CO<sub>2</sub> treatment and all three activity traits in the CNS, in comparison to all of the genes in the CNS.

### 3.5 OA-affected genes and their functions

Genes affected by elevated CO<sub>2</sub> and correlated with OA-induced behavioural change were identified in seven main functions: neurotransmission; cell cycle; cell proliferation and differentiation; neural wiring; transcription, RNA processing and protein processing; immune function; oxidative stress.

#### 3.5.1 Neurotransmission

A range of genes and functional categories involved in various types of neurotransmission were significantly affected by CO<sub>2</sub> treatment (Table 2). We identified small, coordinated downregulation of genes belonging to a cluster of nine functional categories in the CNS, and upregulation of two functional categories in the eyes, involved in ligand-gated ion channel-mediated neurotransmission. The genes contributing most to the up/down-regulation of each of these functional categories (core enrichment genes) in the CNS and eyes included genes for components of acetylcholine, GABA<sub>A</sub> and glutamate ion channel receptors (Table S11). There was also small, coordinated downregulation in the CNS of genes belonging to two functional categories involved in G protein-coupled receptor (GPCR)-mediated neurotransmission, including genes coding for components of metabotropic glutamate, GABA<sub>B</sub>, serotonin and dopamine receptors (Table S12). Notably, a subunit of nicotinic acetylcholine receptors (*chrna10*) was correlated with CO<sub>2</sub> treatment and behaviours in both tissues. *Chrna10* as well as other genes coding for nicotinic acetylcholine receptor subunits (*chrna1*, *chrna3*, *chrna5*, and *chrbn1*) were core enrichment genes in eight functional categories significantly affected by CO<sub>2</sub> treatment in both tissues. Genes coding for regulation of GABAergic neurotransmission were upregulated in both tissues (CNS: *syvn1-b*, eyes: *slc18a2*), and positively correlated with CO<sub>2</sub> treatment and behaviours in the CNS (*phf24*, *rac1*), while *aldh5a1*, which is involved in the final degradation step of GABA (Kim *et al.*, 2009), was negatively correlated with CO<sub>2</sub> treatment and behaviours in the CNS. Furthermore, there was upregulation of *folh1* (glutamate synthesis) and downregulation of *celsr3* (mediator of glutamatergic synapse formation) in the CNS. There was also upregulation in the eyes of two key genes involved in monoaminergic (dopamine, serotonin (5-HT), norepinephrine, and epinephrine) neurotransmission (*maoa*, *slc18a2*).

Genes involved in the general processes required for synaptic neurotransmission also displayed altered expression after elevated CO<sub>2</sub> exposure (Table 2). There was small, coordinated downregulation in the CNS of genes belonging to a cluster of seven functional categories involved in K<sup>+</sup>, Ca<sup>2+</sup> and Na<sup>+</sup> ion transport important for general processes involved in neurotransmission, including maintenance of membrane potential, action potential generation and neurotransmitter release (Table S13). Furthermore, genes involved in regulating synaptic neurotransmission (*futsch*, *dgkq*) were negatively correlated with CO<sub>2</sub> treatment and activity traits in the CNS.

### 3.5.2 Cell cycle

In the CNS, we found small, coordinated upregulation of genes belonging to functional categories involved in the cell cycle, and genes positively correlated with CO<sub>2</sub> treatment and all three activity traits were enriched for cell cycle functional categories (Table 3, Figures 3 and 5). This included genes and functional categories involved in regulating the cell cycle, as well as those specifically involved in the cell cycle stages of interphase and mitosis. In particular, there was small, coordinated upregulation of genes belonging to the functional categories ‘chromosome’ and ‘protein kinase binding’ (Figure 3), and these same functions were enriched in the genes positively correlated with CO<sub>2</sub> treatment and all three activity traits (Figure 5).

### 3.5.3 Cell proliferation and differentiation

Genes involved in cell proliferation and differentiation, including specifically for neuronal differentiation and neurogenesis were mostly positively correlated with CO<sub>2</sub> treatment and behaviours in the CNS (Table 3). Genes involved in neuronal differentiation (*ttc3*), neural stem cell self-renewal (*srvt*), neural progenitor proliferation (*melk*), and neurogenesis (*ncaph*, *adgrb3*) were all positively correlated with CO<sub>2</sub> treatment and activity traits. *Bcar3*, which promotes cell proliferation, migration and redistribution of actin fibres, and *psap*, which acts as a neurotrophic and myelinotrophic factor, were negatively correlated with CO<sub>2</sub> treatment and positively correlated with number of exploratory interactions in the CNS. Several *cdk10* transcripts were identified as correlated with CO<sub>2</sub>-induced behavioural change. *Cdk10* codes for a protein kinase that plays pivotal roles in controlling a range of fundamental cellular processes including cell proliferation and neurogenesis (reviewed in Guen *et al.* (2017)).

### 3.5.4 Neural wiring

A range of genes and functional categories involved in neural wiring, including cell migration and adhesion, and neurite growth and synapse formation were affected by CO<sub>2</sub> treatment, also mostly exhibiting an upregulation in the CNS (Table 3). There was small, coordinated upregulation of genes involved in cell migration functional categories, including ‘motor activity’, ‘actin binding’, ‘cell adhesion’ and ‘integrin complex’. Those genes positively correlated with CO<sub>2</sub> treatment and all three activity traits in the CNS were enriched for similar functional categories: ‘actin filament binding’, ‘myosin complex’, ‘myofibril’, ‘motor activity’ and ‘ruffle membrane’. Genes with a role specifically in neuron migration and adhesion, and the related processes of dendrite and axon outgrowth and branching, dendritic spine formation, and synapse formation were also positively correlated with CO<sub>2</sub> treatment and activity (*rac1*, *ptpr*, *adgrb3*, *apbb1*). One gene involved in neurite growth and branching (*futsch*) was negatively correlated with CO<sub>2</sub> treatment and activity traits.

### 3.5.5 Transcription, RNA processing, and protein processing

There was generally an upregulation of genes and functional categories involved in transcription, RNA processing and protein processing in the CNS, and to a smaller extent in the eyes (Table 4). In the CNS, there was small, coordinated upregulation of genes belonging to functional categories involved in transcription, including ‘DNA duplex unwinding’, and its’ daughter term ‘3’-5’ DNA helicase activity’ was enriched in those genes positively correlated with CO<sub>2</sub> treatment and all three activity traits (Figure 5). There was small, coordinated upregulation in the CNS of genes belonging to the functional category ‘nuclear pore’, and ‘nuclear pore’ was also enriched for those genes positively correlated with CO<sub>2</sub> treatment and all three activity traits in the CNS (Figure 5). Genes involved in transcription were also DE; *nme6*, *chrac1* and

*znf271* were upregulated in the CNS, and *gtf2e2* downregulated in the eyes. There was small, coordinated upregulation of genes involved in ‘RNA processing’, ‘mRNA processing’ and ‘rRNA processing’, as well as functional categories involved in the processes and components of the spliceosome, which excises introns to produce mature mRNA (Figure 3). Components of the spliceosome (*snrpa*, *snrnp200*) were also identified as correlated with CO<sub>2</sub> treatment and behaviours (Table 4).

A range of genes and functional categories involved in protein synthesis, folding and degradation/turnover were significantly upregulated in the CNS, and some were also upregulated in the eyes. Small, coordinated upregulation of genes involved in the initiation and process of translation as well as in functional categories for ribosomal components occurred in both tissues (Figure 3). Genes with similar functions were also positively correlated with CO<sub>2</sub> treatment and activity traits in the CNS, including translation initiation factors (*eif3b*, *eif3d*), an elongation factor (*eef1g*), and ribosomal components (*rpl23a*, *rpl4*, *rpl7l*, *rps27a*). Genes involved in protein translocation (*stt3a*, *rpn1*, *rpn2*, *tmed2*), and protein folding and quality control (*pdia3*, *pdia4*, *pdia5*, *hspa5*) were correlated with CO<sub>2</sub> treatment and behaviours in the CNS. The endoplasmic reticulum associated degradation (ERAD) pathway involves protein ubiquitination followed by proteasomal degradation and we found a range of genes involved in this process to be affected by CO<sub>2</sub> treatment. There was small, coordinated upregulation of genes in the ‘endoplasmic reticulum’ and five ubiquitin-related functional categories in the CNS, of ‘proteasome complex’ in both tissues, and of ‘peptide metabolic process’ in the eyes. Genes positively correlated with CO<sub>2</sub> treatment and all three activity traits were enriched for ‘endoplasmic reticulum lumen’ and included genes coding for E3 ubiquitin ligases (*cblb*, *ttc3*) and a subunit for the 26S proteasome (*rpn1*). A gene coding for an E3 ubiquitin ligase (*syvn1-b*) was also upregulated in the CNS. Lysosomal degradation is another method for protein turnover, and a gene essential for lysosomal function (*ykt6*) was upregulated in both the CNS and eyes.

### 3.5.6 Immune function

Genes and functional categories involved in the three stages of the innate immune response (sensing, signalling and effectors), were affected by CO<sub>2</sub> treatment in both tissues (Table 5). In the eyes, the immune sensor molecule *pglyrp2* was downregulated, while there was small, coordinated upregulation of genes belonging to the functional category ‘scavenger receptor activity’ which binds pathogens. Genes that mediate the immune response via cellular signalling pathways were DE, including upregulation of *map4k5/3* and *syvn1-b*, and downregulation of *psenen* in the CNS. In the eyes, there was upregulation of *maoa*, which plays a key role, via norepinephrine signalling, in the molluscan neuroendocrine-immune axis-like pathway (Liu *et al.*, 2018; Sun *et al.*, 2021; Zhou *et al.*, 2011). Genes involved in the activation and production of immune effectors were also affected by CO<sub>2</sub> treatment. In particular, *tf* coding for transferrin, which sequesters iron so it is unavailable for pathogens and is a key component of the molluscan innate immune response, including in squid (Herath *et al.*, 2015; Lambert *et al.*, 2005; Li *et al.*, 2019; Ong *et al.*, 2006; Salazar *et al.*, 2015), was upregulated and positively correlated with CO<sub>2</sub> treatment and activity traits in the CNS. The key molecular marker of autophagy, *map1l3ca/b*, which plays an important role in the molluscan immune response (Han *et al.*, 2019; Moreau *et al.*, 2015; Picot *et al.*, 2019) was downregulated in the CNS. There was also small, coordinated upregulation of genes belonging to functional categories involved in mediating phagocytosis, including ‘cell adhesion’ and ‘integrin complex’. Genes involved in cell adhesion as part of the immune response (*itga4*, *itga9*, *rac1*, *ptpr*) were also positively correlated with CO<sub>2</sub> treatment and activity traits. The cytoskeleton is also important for phagocytosis and there was small, coordinated upregulation of genes in three cytoskeleton-related functional categories in the CNS (‘motor activity’, ‘actin binding’, and ‘microtubule cytoskeleton’), and two downregulated in the eyes (‘cytoskeleton’ and ‘intermediate filament cytoskeleton organisation’) (Figure 4).

### 3.5.7 Oxidative stress

Genes involved in regulating reactive oxygen species (ROS) and antioxidant production were differentially expressed in both tissues; *tf* (CNS: upregulated and positively correlated with CO<sub>2</sub> treatment and activity traits), *cyb561d2* (CNS: downregulated), *cbs* (eyes: upregulated). Furthermore, *scl4a11*, which regulates the oxidative stress response, was positively correlated with CO<sub>2</sub> treatment and activity traits in the CNS, and

there was small, coordinated downregulation in the CNS of genes involved in ‘glutathione metabolic process’ (Table 6). Genes and functional categories involved in response to oxidative damage were also affected by CO<sub>2</sub> treatment (Table 6). Genes involved in DNA repair were generally upregulated with CO<sub>2</sub> treatment in the CNS; *chrac1* was significantly upregulated, there was small, coordinated upregulation of ‘damaged DNA binding’ and ‘DNA repair’, *spt16*, *foxm1*, *bptf*, and *arpc5* were positively correlated with CO<sub>2</sub> treatment and activity traits, and *nit1*, whose loss of expression promotes resistance to DNA damage stress, was negatively correlated with CO<sub>2</sub> treatment and activity traits. Genes involved in protein damage control and endoplasmic reticulum stress were also affected by CO<sub>2</sub> treatment; *ykt6*, which is essential for autophagy was upregulated in the CNS and eyes, and the heat shock protein *hspa5*, which is a key repressor of the unfolded protein response was positively correlated with CO<sub>2</sub> treatment and activity traits. Furthermore, genes that induce apoptosis in response to DNA damage (*apbb5*) and ER stress (*tmem214-b*), were positively correlated with CO<sub>2</sub> treatment and activity traits. There was also small, coordinated upregulation in the CNS of genes involved in the ‘regulation of apoptotic process’.

#### 4. Discussion

As the nervous system forms the fundamental link between animals and the environments they inhabit (Kelley *et al.*, 2018; O’Donnell, 2018), understanding the neurobiological impacts of environmental change is key to predicting how and why animals will respond to anthropogenic climate change. In this study, we sought to understand how projected end-of-century CO<sub>2</sub> levels alter the nervous system at a molecular level, and how such changes may affect behaviour of the whole animal. To do this, we investigated the transcriptomic response to ocean acidification (OA) of the central and peripheral nervous system of a marine invertebrate with a complex nervous system, the two-toned pygmy squid *Idiosepius pygmaeus*. We then correlated patterns of gene expression with CO<sub>2</sub> treatment levels and OA-affected behaviours in the same individuals. The central nervous system (CNS) and eyes of *I. pygmaeus* responded to elevated CO<sub>2</sub> with significant differential expression (DE) of a small number of genes, and widespread small, coordinated changes of genes belonging to important functional categories between CO<sub>2</sub> conditions. Furthermore, we identified 169 genes in the CNS, six genes in the eyes and ten genes in both tissues that were correlated with CO<sub>2</sub> treatment and one or more behaviours affected by OA, indicating these genes potentially contribute to OA-induced behavioural changes.

The GABA hypothesis is the predominant mechanistic explanation for OA-induced behavioural changes in fish (Nilsson *et al.*, 2012; Tresguerres & Hamilton, 2017) and may also apply to marine invertebrates (Thomas *et al.*, 2020). Pharmacological work has supported the GABA hypothesis in marine molluscs (Clements *et al.*, 2017; Watson *et al.*, 2014), including in *I. pygmaeus* (Thomas *et al.*, 2021). In the whole-body of a pteropod mollusc, a GABA<sub>A</sub> receptor transcript was upregulated after OA exposure (Moya *et al.*, 2016). In fish nervous tissue, OA exposure has variable effects on GABA<sub>A</sub> R subunit transcript expression, causing upregulation in some species (Cohen-Rengifo *et al.*, 2022; Schunter *et al.*, 2018) but not another (Williams *et al.*, 2019). Furthermore, differences in OA exposure duration (Kang *et al.*, 2022; Schunter *et al.*, 2018; Schunter *et al.*, 2016) and magnitude (Toy *et al.*, 2022) are associated with variable effects on the expression of genes coding for GABA<sub>A</sub> R subunits within species. In *I. pygmaeus*, we found small, coordinated downregulation in the CNS and upregulation in the eyes of genes for ion-channel receptors, which included GABA<sub>A</sub> receptor subunit transcripts. In the CNS, there was also upregulation of *syvn1-b* (implicated in GABA<sub>A</sub>α1 receptor subunit degradation (Crider *et al.*, 2014; Jiao *et al.*, 2017)), regulators of GABAergic neurotransmission were positively correlated with CO<sub>2</sub> treatment and behaviours (*phf24*, *rac1*), and *aldh5a1* (involved in the final degradation step of GABA (Kim *et al.*, 2009)) was negatively correlated with CO<sub>2</sub> treatment and behaviours. Together, this data suggests an effect of OA on GABAergic signalling may be widespread, occurring not only in fish but also marine molluscs, however, effects may be species and tissue-specific.

Recent research suggests that various other types of neurotransmission may also be affected by OA and potentially contribute to consequent behavioural responses. Pharmacological research has identified altered function of a range of different types of ligand-gated Cl<sup>-</sup> channels in *I. pygmaeus* (Thomas *et al.*, 2021) and

the dopamine D1 receptor in a damselfish (Hamilton *et al.*, 2023) contributing to OA-induced behavioural changes. Elevated CO<sub>2</sub> upregulated glycinergic, cholinergic and glutamatergic transcripts in the whole body of a pteropod mollusc (Moya *et al.*, 2016), upregulated glutamatergic transcripts in the non-nervous tissue of oysters (Ertl *et al.*, 2016; Wang *et al.*, 2020), and altered acetylcholine receptor transcript expression in the whole body of another pteropod mollusc (Johnson & Hofmann, 2017). In fish nervous tissue, exposure to OA conditions caused upregulation of genes coding for glutamatergic and cholinergic neurotransmission of some species (Cohen-Rengifo *et al.*, 2022; Schunter *et al.*, 2018; Williams *et al.*, 2019), but downregulation in others (Kang *et al.*, 2022; Porteus *et al.*, 2018). In *I. pygmaeus*, we identified small, coordinated downregulation in the CNS and upregulation in the eyes of genes involved in neurotransmission mediated by ligand-gated ion channels, including transcripts for subunits of ionotropic glutamate, glycine and acetylcholine receptors. There was also small, coordinated downregulation in the CNS of G protein-coupled receptor (GPCR)-mediated neurotransmission, including genes for subunits of metabotropic glutamate, serotonin, dopamine and GABA (GABA<sub>B</sub>) receptors. Key genes for glutamatergic and monoaminergic signalling were DE, and a subunit of nicotinic acetylcholine receptors (*chrna10*) was correlated with CO<sub>2</sub> treatment and behaviours in both tissues. Overall, this suggests that OA not only impacts GABA<sub>A</sub> R function, but various different types of neurotransmission mediated by ligand-gated ion channels and GPCRs. However, as with GABAergic signalling, OA effects on other types of neurotransmission may vary by species and tissue type, and possibly other factors such as the magnitude and duration of OA exposure. Further experimentation is needed to understand how OA-induced transcriptomic responses translate to neurotransmission function and behaviour.

Genes involved in the general processes required for synaptic neurotransmission were attenuated in the CNS of *I. pygmaeus* after OA exposure, including Ca<sup>2+</sup>, K<sup>+</sup> and Na<sup>+</sup> ion channels required for maintenance of membrane potential, action potential generation and neurotransmitter release. There was also a negative correlation between the expression of genes regulating synaptic neurotransmission with CO<sub>2</sub> treatment and activity traits. Genes for Ca<sup>2+</sup> and K<sup>+</sup> transporters and the regulation of neurotransmitter release were also downregulated in the brain of spiny damselfish collected from CO<sub>2</sub> seeps (Kang *et al.*, 2022), but upregulated after acute and developmental OA exposure (Schunter *et al.*, 2018), and in fish olfactory tissue after short-term (Williams *et al.*, 2019) and transgenerational OA exposure (Cohen-Rengifo *et al.*, 2022). These transcriptomic signatures suggest an even more widespread effect of OA on neurotransmission, potentially altering the general processes required for synaptic neurotransmission to occur. However, experimentation is required to determine functional effects.

Neuroplasticity is the ability of the nervous system to change. Both neurogenesis (the process by which new neurons are generated and integrated into existing neural circuits) and synaptic plasticity (changing of synaptic strength over time) contribute to neuroplasticity (Costandi, 2016). In the CNS of *I. pygmaeus* we found small, coordinated upregulation and positive correlation with CO<sub>2</sub> treatment and activity traits of genes involved in all the stages required for neurogenesis (re-entering and exiting the cell cycle, cell proliferation and differentiation to form new neurons, and neural wiring involving cell migration and adhesion for new neurons to be incorporated into existing circuits). Widespread upregulation and positive correlations with CO<sub>2</sub> treatment and behaviours of genes in the CNS of *I. pygmaeus* involved in transcription, RNA processing, and protein processing could potentially be a response to deal with the changed protein demand required due to increased neuroplasticity. Notably, *cdk10*, which plays an important role in neurogenesis (Yeh *et al.*, 2013) was identified as correlated with the OA-induced increase in exploratory interactions in both the CNS and eyes. Genes involved in synaptogenesis (the formation of new synapses) and synaptic plasticity were also positively correlated with CO<sub>2</sub> treatment and OA-affected behaviours in the CNS of *I. pygmaeus*.

Despite not assessing the nervous tissue specifically, transcripts involved in neuronal cell adhesion, neuronal differentiation and survival and synaptic plasticity were also upregulated in the whole body of a pteropod mollusc after OA exposure (Moya *et al.*, 2016). In fish nervous tissue, genes involved in neurogenesis were upregulated in some species but not others (Lai *et al.*, 2017), and genes involved in synaptic plasticity were upregulated in some species (Cohen-Rengifo *et al.*, 2022; Schunter *et al.*, 2018), but downregulated in another species (Porteus *et al.*, 2018). Thus, OA-induced transcriptomic responses related to neuroplasticity may

be widespread, occurring in fish and marine molluscs. However, this response may be taxa-specific and/or could be affected by differences in CO<sub>2</sub> exposure duration and magnitude that have differed between studies.

Elevated CO<sub>2</sub> alters the molluscan immune response, with most research focusing on bivalves (Bibby *et al.*, 2008; Liet *et al.*, 2015; Liu *et al.*, 2016; Su *et al.*, 2018; Wu *et al.*, 2016), though the immune response of an octopus was also affected by elevated CO<sub>2</sub> (Culler-Juarez & Onthank, 2021). Here, we found DE of genes that regulate immune signal transduction pathways and which are also implicated in the molluscan immune response (*map4k5/3*, *syvn1-b*, *psenen*, *cbs*) (Canesi *et al.*, 2006; De Zoysa *et al.*, 2010; Goodson *et al.*, 2005; Salazar *et al.*, 2015). There were also changes in expression of a range of genes that code for immune effectors, including iron sequestration (*tf* and *cbs*), autophagy (*map1l3ca/b*), controlling the pool of available nucleoside triphosphates (*nme6*), and phagocytosis ('cell adhesion' and multiple cytoskeleton functional categories). Previous research has also indicated altered phagocytosis in molluscs at elevated CO<sub>2</sub>; adhesion capacity of haemocytes was decreased in a clam and expression of integrin (involved in cell adhesion for phagocytosis) was decreased in an oyster species (Ivanina *et al.*, 2014) and increased in another oyster (Ertl *et al.*, 2016). Furthermore, the phagocytic rate and cytoskeleton component abundance was decreased, and the expression of cytoskeleton genes was upregulated, in a clam at elevated CO<sub>2</sub> (Su *et al.*, 2018). Our results show an effect of OA on the transcriptional profile of genes implicated in the immune response suggesting OA-induced alterations in immune function may also occur in molluscan nervous tissue, though further research directly measuring immune function within the nervous system is required.

Cross-talk between the neuroendocrine and immune systems coordinates appropriate physiological and behavioural responses to environmental change (Demas *et al.*, 2011). In molluscs, neuronal release of norepinephrine regulates immune responses through a neuroendocrine-immune axis-like pathway (Liu *et al.*, 2017). Specifically, changes in the expression and activity of *maoa* (upregulated in *I. pygmaeus* eyes here) plays a key role in immune functioning via norepinephrine in molluscs (Liu *et al.*, 2018; Sun *et al.*, 2021; Zhou *et al.*, 2011). Immune-derived factors can also feedback to alter the nervous system and behaviour (Adamo, 2006; Dantzer & Kelley, 2007). Indeed, *tf*, which is a key component of the molluscan innate immune response (Lambert *et al.*, 2005; Ong *et al.*, 2006; Herath *et al.*, 2015; Salazar *et al.*, 2015; Li *et al.*, 2019) was upregulated and positively correlated with CO<sub>2</sub> treatment and activity traits in the CNS of *I. pygmaeus*. We also found the expression of genes coding for integrins *itga4* and *itga9*, cell adhesion molecules playing a key role in invertebrate immune responses (Johansson, 1999; Terahara *et al.*, 2006), were positively correlated in the CNS with CO<sub>2</sub> treatment and activity traits. Therefore, it is possible that OA-induced changes in neurotransmission could have consequences on immune function, and changes in immune function could also feedback on the nervous system to alter behaviours at elevated CO<sub>2</sub>. However, the potential links between OA, neurotransmission, immune function and behaviour remain to be experimentally tested.

Oxidative stress occurs when there is an imbalance between the production of reactive oxygen species (ROS) and protection by antioxidant mechanisms (Halliwell & Gutteridge, 2015). Elevated CO<sub>2</sub> induces oxidative stress in molluscs, increasing ROS and altering antioxidant defences inducing DNA damage, lipid peroxidation and apoptosis (Cao, Liu, *et al.*, 2018; Cao, Wang, *et al.*, 2018; Kim *et al.*, 2023; Tomanek *et al.*, 2011; Wang *et al.*, 2016; Zhang *et al.*, 2021). In *I. pygmaeus*, we found DE of genes implicated in the production of antioxidants, including ascorbate and glutathione. We also identified upregulation in the CNS of genes involved in DNA damage and repair, protein damage and endoplasmic reticulum stress, and cellular stress-induced apoptosis. In molluscs, OA exposure has previously been shown to result in DNA damage (Cao, Liu, *et al.*, 2018; Nardi *et al.*, 2018) and increased apoptosis (Cao, Liu, *et al.*, 2018; Zhang *et al.*, 2021).

The nervous system is particularly vulnerable to oxidative stress (Halliwell, 2006; Valko *et al.*, 2007) and oxidative stress-induced damage within the nervous system can disrupt neurotransmission and neuronal function (Bouayed *et al.*, 2009; Halliwell, 2006; Halliwell & Gutteridge, 2015; Lebel & Bondy, 1991). In mammals, a link between oxidative stress in the nervous system and changes in behaviour has been demonstrated (Bhatt *et al.*, 2020; Bouayed, 2011; Rammal *et al.*, 2010). In the CNS of *I. pygmaeus*, we identified a positive correlation between the expression of genes implicated in oxidative stress and CO<sub>2</sub> treatment and OA-affected

behaviours. In the eyes, two genes (*crb*, *zranb1*) potentially correlated with OA-induced behavioural alterations of *I. pygmaeus* are implicated in oxidative-stress induced retinal degeneration (Chartier *et al.*, 2012; Wang *et al.*, 2018). In particular, *crb* prevents photoreceptor degeneration by limiting the production of ROS and the resultant oxidative damage (Chartier *et al.*, 2012). A recent study in a cuttlefish found the behavioural effects of OA were associated with an altered retinal structure and an increase in apoptotic cells within the eyes (Xie *et al.*, 2023). Thus, it's possible that OA-induced oxidative stress could contribute to behavioural alterations at elevated CO<sub>2</sub>, potentially through central and peripheral mechanisms, but further electrophysiological and whole-animal behavioural experimentation is required.

When interpreting our results, there are a few important things to consider. Firstly, despite the reasonable assumption that changes in gene expression driving behavioural responses occur prior to behavioural production (Fischer *et al.*, 2021), we measured gene expression immediately after the OA-induced behavioural responses in *I. pygmaeus* due to the necessity of terminal sampling to obtain nervous tissue. Furthermore, the process of transcribing genes is far too slow to mediate rapid behavioural responses, which are instead mediated by fast electrical signals passed along and between neurons (Fischer *et al.*, 2021). Thus, our transcriptomic results do not describe the neuronal mechanisms driving the immediate behavioural responses to a stimulus, but rather those that likely contribute to longer-term changes in behaviour (Clayton *et al.*, 2020; Fischer *et al.*, 2021) in OA conditions. Secondly, organism responses to OA can be sex-specific (Ellis *et al.*, 2017), including marine invertebrate behavioural responses (Marčeta *et al.*, 2020; Richardson *et al.*, 2021). We used males only in this study. Future research could consider using both sexes to determine whether behavioural responses to OA are sex-specific, and if so whether differing transcriptional profiles underly these sex-specific responses.

## Conclusions

Here, we demonstrate differential expression of specific genes and widespread small, coordinated changes in expression of genes belonging to relevant functional categories in the CNS and eyes following short-term exposure of male *I. pygmaeus* to OA. We also report genes correlated with both CO<sub>2</sub> treatment and OA-affected behaviours, indicating these genes as potentially correlated with CO<sub>2</sub>-induced behavioural change in *I. pygmaeus*. The results identify alterations in the transcriptional profile of genes implicated in neurotransmission, neuroplasticity, immune function and oxidative stress. These molecular changes may contribute to OA-induced behavioural change, as suggested by correlations between gene expression profiles, CO<sub>2</sub>treatment and OA-affected behaviours. Our results build on existing knowledge and provide novel hypotheses for future experiments, including electrophysiological and behavioural tests, to determine the range of processes responsible for behavioural changes in marine animals exposed to projected future OA conditions.

## Acknowledgements

We thank the technical staff at James Cook University Marine and Aquaculture Facilities Unit (Ben Lawes, Simon Wever and Andrew Thompson), and Annam Raza, Natalie Swinhoe and Michael Jarrold for assistance with the live animal work. We also thank the Breakwater Marina, Townsville for permission to collect animals within their premises. Thank you to Carolyn Smith-Keune and Paul O'Brien for molecular laboratory support and Taewoo Ryu for advice on the computational analysis. We are grateful for the support provided by the Scientific Computing and Data Analysis section of Research Support Division at Okinawa Institute of Science and Technology Graduate University.

## Funding

This work was supported by the Australian Research Council Centre of Excellence for Coral Reef Studies (PLM, S-AW), an Australian Government Research Training Program Scholarship (JTT) and the Okinawa Institute of Science and Technology Graduate University (TR, RH, JTT).

## Data Accessibility

Raw RNA-sequencing and ISO-sequencing data, and the transcriptome assembly (fasta file) can be found at

NCBI BioProject PRJNA798187 (this is embargoed until peer-reviewed publication) (Thomas *et al.*, 2022). Raw gene count data, raw water sampling data, all scripts used for bioinformatic analyses, the annotated transcriptome assembly (OmicsBox and csv files), R code used for the statistical analyses (differential expression and gene set analyses), and data files to accompany the statistical analyses are available from DOI 10.25903/ha66-mm11 (this DOI is embargoed until peer-reviewed publication) (Thomas *et al.*, 2023b). All R code for the statistical analyses (correlating gene expression profiles with CO<sub>2</sub> treatment and OA-affected behaviours), as well as accompanying data files for the statistical analyses, can be found at DOI 10.25903/7dcz-th66 (this DOI is embargoed until peer-reviewed publication) (Thomas *et al.*, 2023a).

### Author Contributions

Jodi Thomas: Conceptualisation, Methodology, Software, Formal analysis, Investigation, Resources, Data curation, Writing - original draft, Writing - review and editing, Visualisation

Roger Huerlimann: Methodology, Software, Writing - review and editing

Celia Schunter: Conceptualisation, Methodology, Resources, Writing - review and editing

Sue-Ann Watson: Conceptualisation, Resources, Writing - review and editing, Supervision

Philip Munday: Conceptualisation, Resources, Writing - review and editing, Supervision

Timothy Ravasi: Conceptualisation, Methodology, Resources, Writing - review and editing, Supervision

### References

- Adamo, S. A. (2006). Comparative psychoneuroimmunology: Evidence from the insects. *Behavioral and Cognitive Neuroscience Reviews*, 5 (3), 128-140. doi:10.1177/1534582306289580
- Andrews, S. (2010). FastQC: A quality control tool for high throughput sequence data. <https://www.bioinformatics.babraham.ac.uk/projects/fastqc/>.
- Bertness, M. D., Gaines, S. D., & Hay, M. E. (2001). *Marine Community Ecology*. Sunderland, Massachusetts: Sinauer Associates.
- Bhatt, S., Nagappa, A. N., & Patil, C. R. (2020). Role of oxidative stress in depression. *Drug Discovery Today*, 25 (7), 1270-1276. doi:<https://doi.org/10.1016/j.drudis.2020.05.001>
- Bibby, R., Widdicombe, S., Parry, H., Spicer, J., & Pipe, R. (2008). Effects of ocean acidification on the immune response of the blue mussel *Mytilus edulis*. *Aquatic Biology*, 2 (1), 67-74.
- Bindoff, N. L., Cheung, W. W., Kairo, J. G., Arístegui, J., Guinder, V. A., Hallberg, R., . . . Williamson, P. (2019). Changing ocean, marine ecosystems, and dependent communities. In H.-O. Pörtner, D. Roberts, V. Masson-Delmotte, P. Zhai, M. Tignor, E. Poloczanska, K. Mintenbeck, A. Alegria, M. Nicolai, A. Okem, J. Petzold, B. Rama, & N. Weyer (Eds.), *IPCC Special Report on the Ocean and Cryosphere in a Changing Climate* (pp. 447 - 587). Cambridge, UK and New York, NY, USA: Cambridge University Press.
- Bouayed, J. (2011). Relationship between oxidative stress and anxiety: Emerging role of antioxidants within therapeutic or preventive approaches. *Anxiety Disorders*, 27-38.
- Bouayed, J., Rammal, H., & Soulimani, R. (2009). Oxidative stress and anxiety: Relationship and cellular pathways. *Oxidative Medicine and Cellular Longevity*, 2, 623654. doi:10.4161/oxim.2.2.7944
- Canesi, L., Betti, M., Ciacci, C., Lorusso, L., Pruzzo, C., & Gallo, G. (2006). Cell signalling in the immune response of mussel hemocytes. *Invertebrate Survival Journal*, 3 (1), 40-49.
- Cao, R., Liu, Y., Wang, Q., Zhang, Q., Yang, D., Liu, H., . . . Zhao, J. (2018). The impact of ocean acidification and cadmium on the immune responses of Pacific oyster, *Crassostrea gigas*. *Fish & Shellfish Immunology*, 81, 456-462. doi:<https://doi.org/10.1016/j.fsi.2018.07.055>

- Cao, R., Wang, Q., Yang, D., Liu, Y., Ran, W., Qu, Y., . . . Zhao, J. (2018). CO<sub>2</sub>-induced ocean acidification impairs the immune function of the Pacific oyster against *Vibrio splendidus* challenge: An integrated study from a cellular and proteomic perspective. *Science of The Total Environment*, *625*, 1574-1583. doi:<https://doi.org/10.1016/j.scitotenv.2018.01.056>
- Charpentier, C. L., & Cohen, J. H. (2016). Acidification and  $\gamma$ -aminobutyric acid independently alter kairomone-induced behaviour. *Open Science*, *3* (9), 160311. doi:10.1098/rsos.160311
- Chartier, F. J.-M., Hardy, É. J.-L., & Laprise, P. (2012). Crumbs limits oxidase-dependent signaling to maintain epithelial integrity and prevent photoreceptor cell death. *Journal of Cell Biology*, *198* (6), 991-998. doi:10.1083/jcb.201203083
- Chen, E. Y.-S. (2021). Often overlooked: Understanding and meeting the current challenges of marine invertebrate conservation. *Frontiers in Marine Science*, *8* (1161), 690704. doi:10.3389/fmars.2021.690704
- Chen, S., Zhou, Y., Chen, Y., & Gu, J. (2018). fastp: an ultra-fast all-in-one FASTQ preprocessor. *Bioinformatics*, *34* (17), i884-i890. doi:10.1093/bioinformatics/bty560
- Chung, W.-S., Kurniawan, N. D., & Marshall, N. J. (2022). Comparative brain structure and visual processing in octopus from different habitats. *Current Biology*, *32* (1), 97-110.e114. doi:<https://doi.org/10.1016/j.cub.2021.10.070>
- Clayton, D. F., Anreiter, I., Aristizabal, M., Frankland, P. W., Binder, E. B., & Citri, A. (2020). The role of the genome in experience-dependent plasticity: Extending the analogy of the genomic action potential. *Proceedings of the National Academy of Sciences*, *117* (38), 23252-23260. doi:10.1073/pnas.1820837116
- Clements, J. C., Bishop, M. M., & Hunt, H. L. (2017). Elevated temperature has adverse effects on GABA-mediated avoidance behaviour to sediment acidification in a wide-ranging marine bivalve. *Marine Biology*, *164* (3), 56. doi:10.1007/s00227-017-3085-1
- Cohen-Rengifo, M., Danion, M., Gonzalez, A.-A., Bégout, M.-L., Cormier, A., Noël, C., . . . Mazurais, D. (2022). The extensive transgenerational transcriptomic effects of ocean acidification on the olfactory epithelium of a marine fish are associated with a better viral resistance. *BMC Genomics*, *23* (1), 448. doi:10.1186/s12864-022-08647-w
- Cooke, S. J., Sack, L., Franklin, C. E., Farrell, A. P., Beardall, J., Wikelski, M., & Chown, S. L. (2013). What is conservation physiology? Perspectives on an increasingly integrated and essential science. *Conservation Physiology*, *1* (1), cot001. doi:10.1093/conphys/cot001
- Costandi, M. (2016). *Neuroplasticity*. Cambridge, Massachusetts: The MIT Press.
- Crider, A., Pandya, C. D., Peter, D., Ahmed, A. O., & Pillai, A. (2014). Ubiquitin-proteasome dependent degradation of GABA<sub>A</sub> $\alpha$ 1 in autism spectrum disorder. *Molecular Autism*, *5* (1), 45. doi:10.1186/2040-2392-5-45
- Culler-Juarez, M. E., & Onthank, K. L. (2021). Elevated immune response in *Octopus rubescens* under ocean acidification and warming conditions. *Marine Biology*, *168* (9), 137. doi:10.1007/s00227-021-03913-z
- Dantzer, R., & Kelley, K. W. (2007). Twenty years of research on cytokine-induced sickness behavior. *Brain, Behavior, and Immunity*, *21* (2), 153-160. doi:<https://doi.org/10.1016/j.bbi.2006.09.006>
- Davidson, N. M., & Oshlack, A. (2014). Corset: Enabling differential gene expression analysis for *de novo* assembled transcriptomes. *Genome Biology*, *15* (7), 1-14.
- De Zoysa, M., Nikapitiya, C., Oh, C., Whang, I., Lee, J.-S., Jung, S.-J., . . . Lee, J. (2010). Molecular evidence for the existence of lipopolysaccharide-induced TNF- $\alpha$  factor (LITAF) and Rel/NF- $\kappa$ B pathways in disk abalone (*Haliotis discus discus*). *Fish & Shellfish Immunology*, *28* (5), 754-763. doi:<https://doi.org/10.1016/j.fsi.2010.01.024>

- Demas, G. E., Adamo, S. A., & French, S. S. (2011). Neuroendocrine-immune crosstalk in vertebrates and invertebrates: Implications for host defence. *Functional Ecology*, *25* (1), 29-39. doi:<https://doi.org/10.1111/j.1365-2435.2010.01738.x>
- Doney, S. C., Fabry, V. J., Feely, R. A., & Kleypas, J. A. (2009). Ocean acidification: The other CO<sub>2</sub> problem. *Annual Review of Marine Science*, *1* (1), 169-192. doi:[10.1146/annurev.marine.010908.163834](https://doi.org/10.1146/annurev.marine.010908.163834)
- Durant, A., Khodikian, E., & Porteus, C. S. (2023). Ocean acidification alters foraging behaviour in Dungeness crab through impairment of the olfactory pathway. *Global Change Biology*, *n/a* (n/a). doi:<https://doi.org/10.1111/gcb.16738>
- Ellis, R. P., Davison, W., Queirós, A. M., Kroeker, K. J., Calosi, P., Dupont, S., . . . Urbina, M. A. (2017). Does sex really matter? Explaining intraspecific variation in ocean acidification responses. *Biology Letters*, *13* (2), 20160761.
- Ertl, N. G., O'Connor, W. A., Wiegand, A. N., & Elizur, A. (2016). Molecular analysis of the Sydney rock oyster (*Saccostrea glomerata*) CO<sub>2</sub> stress response. *Climate Change Responses*, *3* (1), 6. doi:[10.1186/s40665-016-0019-y](https://doi.org/10.1186/s40665-016-0019-y)
- Ewels, P., Magnusson, M., Lundin, S., & Käller, M. (2016). MultiQC: Summarize analysis results for multiple tools and samples in a single report. *Bioinformatics*, *32* (19), 3047-3048. doi:[10.1093/bioinformatics/btw354](https://doi.org/10.1093/bioinformatics/btw354)
- Fischer, E. K., Hauber, M. E., & Bell, A. M. (2021). Back to the basics? Transcriptomics offers integrative insights into the role of space, time and the environment for gene expression and behaviour. *Biology Letters*, *17* (9), 20210293. doi:[10.1098/rsbl.2021.0293](https://doi.org/10.1098/rsbl.2021.0293)
- Fuller, A., Dawson, T., Helmuth, B., Hetem, Robyn S., Mitchell, D., & Maloney, Shane K. (2010). Physiological mechanisms in coping with climate change. *Physiological and Biochemical Zoology*, *83* (5), 713-720. doi:[10.1086/652242](https://doi.org/10.1086/652242)
- Fuller, T. F., Ghazalpour, A., Aten, J. E., Drake, T. A., Lusic, A. J., & Horvath, S. (2007). Weighted gene coexpression network analysis strategies applied to mouse weight. *Mammalian Genome*, *18* (6), 463-472.
- González, I., Déjean, S., Martin, P., & Baccini, A. (2008). CCA: An R package to extend canonical correlation analysis. *Journal of Statistical Software*, *23* (12), 1-14.
- Goodson, M. S., Kojadinovic, M., Troll, J. V., Scheetz, T. E., Casavant, T. L., Soares, M. B., & McFall-Ngai, M. J. (2005). Identifying components of the NF- $\kappa$ B pathway in the beneficial *Euprymna scolopes* - *Vibrio fischeri* light organ symbiosis. *Applied and Environmental Microbiology*, *71* (11), 6934-6946. doi:[10.1128/AEM.71.11.6934-6946.2005](https://doi.org/10.1128/AEM.71.11.6934-6946.2005)
- Guen, V. J., Gamble, C., Lees, J. A., & Colas, P. (2017). The awakening of the CDK10/Cyclin M protein kinase. *Oncotarget*, *8* (30), 50174-50186. doi:[10.18632/oncotarget.15024](https://doi.org/10.18632/oncotarget.15024)
- Halliwell, B. (2006). Oxidative stress and neurodegeneration: Where are we now? *Journal of Neurochemistry*, *97* (6), 1634-1658. doi:<https://doi.org/10.1111/j.1471-4159.2006.03907.x>
- Halliwell, B., & Gutteridge, J. (2015). Oxidative stress and redox regulation: Adaptation, damage, repair, senescence, and death. In B. Halliwell & J. Gutteridge (Eds.), *Free Radicals in Biology and Medicine. Fifth Edition* (Vol. 3, pp. 199-283): Oxford University Press.
- Hamilton, T. J., Tresguerres, M., Kwan, G. T., Szaskiewicz, J., Franczak, B., Cyrokak, T., . . . Kline, D. I. (2023). Effects of ocean acidification on dopamine-mediated behavioral responses of a coral reef damselfish. *Science of The Total Environment*, 162860. doi:<https://doi.org/10.1016/j.scitotenv.2023.162860>
- Han, Z., Wang, W., Lv, X., Zong, Y., Liu, S., Liu, Z., . . . Song, L. (2019). ATG10 (autophagy-related 10) regulates the formation of autophagosome in the anti-virus immune response of pacific oyster (*Crassostrea gigas*). *Fish & Shellfish Immunology*, *91*, 325-332. doi:<https://doi.org/10.1016/j.fsi.2019.05.027>

- Hanlon, R. T., & Messenger, J. B. (2018). *Cephalopod Behaviour*(Second ed.). Cambridge: Cambridge University Press.
- Hannan, K. D., Miller, G. M., Watson, S.-A., Rummer, J. L., Fabricius, K., & Munday, P. L. (2020). Diel  $p$  CO<sub>2</sub> variation among coral reefs and microhabitats at Lizard Island, Great Barrier Reef. *Coral Reefs*, *39* (5), 1391-1406. doi:10.1007/s00338-020-01973-z
- Herath, H. M. L. P. B., Elvitigala, D. A. S., Godahewa, G. I., Whang, I., & Lee, J. (2015). Molecular insights into a molluscan transferrin homolog identified from disk abalone (*Haliotis discus discus*) evidencing its detectable role in host antibacterial defense. *Developmental & Comparative Immunology*, *53* (1), 222-233. doi:https://doi.org/10.1016/j.dci.2015.07.013
- Heuer, R. M., Hamilton, T. J., & Nilsson, G. E. (2019). The physiology of behavioural impacts of high CO<sub>2</sub>. In M. Grosell, P. L. Munday, A. P. Farrell, & C. J. Brauner (Eds.), *Carbon Dioxide*(Vol. 37, pp. 161-194). Cambridge, San Diego, Oxford, London: Academic Press.
- Horvath, S., & Dong, J. (2008). Geometric interpretation of gene coexpression network analysis. *PLoS Computational Biology*, *4* (8), e1000117-e1000117. doi:10.1371/journal.pcbi.1000117
- Ivanina, A. V., Hawkins, C., & Sokolova, I. M. (2014). Immunomodulation by the interactive effects of cadmium and hypercapnia in marine bivalves *Crassostrea virginica* and *Mercenaria mercenaria*. *Fish & Shellfish Immunology*, *37* (2), 299-312. doi:https://doi.org/10.1016/j.fsi.2014.02.016
- Jackson, G. D. (1988). The use of statolith microstructures to analyze life history events in the small tropical cephalopod *Idiosepius pygmaeus*. *Fishery Bulletin*, *87*, 265-272.
- Jiao, D., Chen, Y., Liu, Y., Ju, Y., Long, J., Du, J., . . . Liu, J. (2017). SYVN1, an ERAD E3 ubiquitin ligase, is involved in GABA<sub>A</sub>α1 degradation associated with methamphetamine-induced conditioned place preference. *Frontiers in Molecular Neuroscience*, *10* (313). doi:10.3389/fnmol.2017.00313
- Johnson, K. M., & Hofmann, G. E. (2017). Transcriptomic response of the Antarctic pteropod *Limacina helicina antarctica* to ocean acidification. *BMC Genomics*, *18* (1), 812. doi:10.1186/s12864-017-4161-0
- Kang, J., Nagelkerken, I., Rummer, J. L., Rodolfo-Metalpa, R., Munday, P. L., Ravasi, T., & Schunter, C. (2022). Rapid evolution fuels transcriptional plasticity to ocean acidification. *Global Change Biology*, *00*, 1-16. doi:https://doi.org/10.1111/gcb.16119
- Kelley, J., Chapuis, L., Davies, W. I. L., & Collin, S. (2018). Sensory system responses to human-induced environmental change. *Frontiers in Ecology and Evolution*, *6*, 95.
- Kim, M. J., Kim, J. A., Lee, D.-W., Park, Y.-S., Kim, J.-H., & Choi, C. Y. (2023). Oxidative Stress and Apoptosis in Disk Abalone (*Haliotis discus hannai*) Caused by Water Temperature and pH Changes. *Antioxidants*, *12* (5), 1003.
- Kim, Y.-G., Lee, S., Kwon, O.-S., Park, S.-Y., Lee, S.-J., Park, B.-J., & Kim, K.-J. (2009). Redox-switch modulation of human SSADH by dynamic catalytic loop. *The EMBO Journal*, *28* (7), 959-968. doi:10.1038/emboj.2009.40
- Kroeker, K. J., Kordas, R. L., Crim, R. N., & Singh, G. G. (2010). Meta-analysis reveals negative yet variable effects of ocean acidification on marine organisms. *Ecology Letters*, *13* (11), 1419-1434. doi:https://doi.org/10.1111/j.1461-0248.2010.01518.x
- Lai, F., Fagernes, C. E., Bernier, N. J., Miller, G. M., Munday, P. L., Jutfelt, F., & Nilsson, G. E. (2017). Responses of neurogenesis and neuroplasticity related genes to elevated CO<sub>2</sub> levels in the brain of three teleost species. *Biology Letters*, *13* (8), 20170240. doi:10.1098/rsbl.2017.0240
- Lambert, L. A., Perri, H., Halbrooks, P. J., & Mason, A. B. (2005). Evolution of the transferrin family: Conservation of residues associated with iron and anion binding. *Comparative Biochemistry and Physiology Part B: Biochemistry and Molecular Biology*, *142* (2), 129-141. doi:https://doi.org/10.1016/j.cbpb.2005.07.007

- Langfelder, P., & Horvath, S. (2008). WGCNA: An R package for weighted correlation network analysis. *BMC Bioinformatics*, 9 (1), 1-13.
- Lebel, C. P., & Bondy, S. C. (1991). Oxygen radicals: Common mediators of neurotoxicity. *Neurotoxicology and Teratology*, 13 (3), 341-346. doi:[https://doi.org/10.1016/0892-0362\(91\)90081-7](https://doi.org/10.1016/0892-0362(91)90081-7)
- Li, H.-W., Chen, C., Kuo, W.-L., Lin, C.-J., Chang, C.-F., & Wu, G.-C. (2019). The characteristics and expression profile of transferrin in the accessory nidamental gland of the bigfin reef squid during bacteria transmission. *Scientific Reports*, 9 (1), 20163. doi:[10.1038/s41598-019-56584-8](https://doi.org/10.1038/s41598-019-56584-8)
- Li, S., Liu, Y., Liu, C., Huang, J., Zheng, G., Xie, L., & Zhang, R. (2015). Morphology and classification of hemocytes in *Pinctada fucata* and their responses to ocean acidification and warming. *Fish & Shellfish Immunology*, 45 (1), 194-202. doi:<https://doi.org/10.1016/j.fsi.2015.04.006>
- Liu, S., Shi, W., Guo, C., Zhao, X., Han, Y., Peng, C., . . . Liu, G. (2016). Ocean acidification weakens the immune response of blood clam through hampering the NF-kappa  $\beta$  and toll-like receptor pathways. *Fish & Shellfish Immunology*, 54 , 322-327. doi:<https://doi.org/10.1016/j.fsi.2016.04.030>
- Liu, Z., Wang, L., Lv, Z., Zhou, Z., Wang, W., Li, M., . . . Song, L. (2018). The cholinergic and adrenergic autocrine signaling pathway mediates immunomodulation in oyster *Crassostrea gigas*. *Frontiers in Immunology*, 9 (284), 284. doi:[10.3389/fimmu.2018.00284](https://doi.org/10.3389/fimmu.2018.00284)
- Liu, Z., Zhou, Z., Jiang, Q., Wang, L., Yi, Q., Qiu, L., & Song, L. (2017). The neuroendocrine immunomodulatory axis-like pathway mediated by circulating haemocytes in pacific oyster *Crassostrea gigas*. *Open Biology*, 7 (1), 160289. doi:[10.1098/rsob.160289](https://doi.org/10.1098/rsob.160289)
- Love, M. I., Huber, W., & Anders, S. (2014). Moderated estimation of fold change and dispersion for RNA-seq data with DESeq2. *Genome Biology*, 15 (12), 550. doi:[10.1186/s13059-014-0550-8](https://doi.org/10.1186/s13059-014-0550-8)
- Marčeta, T., Matozzo, V., Alban, S., Badocco, D., Pastore, P., & Marin, M. G. (2020). Do males and females respond differently to ocean acidification? An experimental study with the sea urchin *Paracentrotus lividus*. *Environmental Science and Pollution Research* , 1-15.
- Mather, J. A. (2006). Behaviour development: A cephalopod perspective. *International Journal of Comparative Psychology*, 19 (1), 98-115.
- Merico, D., Isserlin, R., Stueker, O., Emili, A., & Bader, G. D. (2010). Enrichment map: A network-based method for gene-set enrichment visualization and interpretation. *PloS One*, 5 (11), e13984.
- Moreau, P., Moreau, K., Segarra, A., Tourbiez, D., Travers, M.-A., Rubinsztein, D. C., & Renault, T. (2015). Autophagy plays an important role in protecting Pacific oysters from OsHV-1 and *Vibrio aestuarianus* infections. *Autophagy*, 11 (3), 516-526. doi:[10.1080/15548627.2015.1017188](https://doi.org/10.1080/15548627.2015.1017188)
- Moya, A., Howes, E. L., Lacoue-Labarthe, T., Forêt, S., Hanna, B., Medina, M., . . . Torda, G. (2016). Near-future pH conditions severely impact calcification, metabolism and the nervous system in the pteropod *Heliconoides inflatus* . *Global Change Biology*, 22 (12), 3888-3900. doi:[10.1111/gcb.13350](https://doi.org/10.1111/gcb.13350)
- Moynihan, M. (1983). Notes on the behavior of *Idiosepius pygmaeus* (Cephalopoda; Idiosepiidae). *Behaviour*, 85 (1), 42-57.
- Muntz, W. R. A. (1999). Visual systems, behaviour, and environment in cephalopods. In S. N. Archer, M. B. A. Djamgoz, E. R. Loew, J. C. Partridge, & S. Vallerga (Eds.), *Adaptive Mechanisms in the Ecology of Vision* (pp. 467-483). Dordrecht: Springer Netherlands.
- Nagelkerken, I., & Connell, S. D. (2015). Global alteration of ocean ecosystem functioning due to increasing human CO2 emissions. *Proceedings of the National Academy of Sciences*, 112 (43), 13272-13277.
- Nagelkerken, I., & Munday, P. L. (2015). Animal behaviour shapes the ecological effects of ocean acidification and warming: Moving from individual to community-level responses. *Global Change Biology*, 22 (3), 974-989.

doi:10.1111/gcb.13167

Nardi, A., Benedetti, M., d'Errico, G., Fattorini, D., & Regoli, F. (2018). Effects of ocean warming and acidification on accumulation and cellular responsiveness to cadmium in mussels *Mytilus galloprovincialis* : Importance of the seasonal status. *Aquatic Toxicology*, *204* , 171-179. doi:<https://doi.org/10.1016/j.aquatox.2018.09.009>

Nilsson, G. E., Dixon, D. L., Domenici, P., McCormick, M. I., Sorensen, C., Watson, S.-A., & Munday, P. L. (2012). Near-future carbon dioxide levels alter fish behaviour by interfering with neurotransmitter function. *Nature Climate Change*, *2* (3), 201-204. doi:10.1038/NCLIMATE1352

O'Donnell, S. (2018). The neurobiology of climate change. *The Science of Nature*, *105* (1), 1-7.

Ong, S. T., Shan Ho, J. Z., Ho, B., & Ding, J. L. (2006). Iron-withholding strategy in innate immunity. *Immunobiology*, *211* (4), 295-314. doi:<https://doi.org/10.1016/j.imbio.2006.02.004>

Patro, R., Duggal, G., Love, M. I., Irizarry, R. A., & Kingsford, C. (2017). Salmon provides fast and bias-aware quantification of transcript expression. *Nature Methods*, *14* (4), 417-419. doi:10.1038/nmeth.4197

Picot, S., Morga, B., Faury, N., Chollet, B., Degremont, L., Travers, M.-A., . . . Arzul, I. (2019). A study of autophagy in hemocytes of the Pacific oyster, *Crassostrea gigas* . *Autophagy*, *15* (10), 1801-1809. doi:10.1080/15548627.2019.1596490

Porteus, C. S., Hubbard, P. C., Webster, T. M. U., van Aerle, R., Canario, A. V., Santos, E. M., & Wilson, R. W. (2018). Near-future CO<sub>2</sub> levels impair the olfactory system of a marine fish. *Nature Climate Change*, *8* (8), 737-746. doi:10.1038/s41558-018-0224-8

Portner, H.-O., Langenbuch, M., & Reipschlag, A. (2004). Biological impact of elevated ocean CO<sub>2</sub> concentrations: Lessons from animal physiology and earth history. *Journal of Oceanography*, *60* (4), 705-718. doi:10.1007/s10872-004-5763-0

R Core Team. (2021). R: A language and environment for statistical computing. Vienna, Austria: R Foundation for Statistical Computing. Retrieved from <https://www.R-project.org/>

Rammal, H., Bouayed, J., & Soulimani, R. (2010). A direct relationship between aggressive behavior in the resident/intruder test and cell oxidative status in adult male mice. *European Journal of Pharmacology*, *627* (1), 173-176. doi:<https://doi.org/10.1016/j.ejphar.2009.11.001>

Reid, A. (2005). Family Idiiosepiidae. In P. Jereb & C. F. E. Roper (Eds.), *Cephalopods of the World : An Annotated and Illustrated Catalogue of Cephalopod Species Known to Date. Volume 1. Chambered Nautilus and Sepioids (Nautilidae, Sepiidae, Sepiolidae, Sepiadariidae, Idiiosepiidae and Spirulidae)*. (Vol. 1, pp. 208 - 210). Rome: FAO.

Richardson, B., Martin, H., Bartels-Hardege, H., Fletcher, N., & Hardege, J. D. (2021). The role of changing pH on olfactory success of predator-prey interactions in green shore crabs, *Carcinus maenas*. *Aquatic Ecology* . doi:10.1007/s10452-021-09913-x

RStudio Team. (2021). RStudio: Integrated development environment for R. PBC, Boston, MA: RStudio. Retrieved from <http://www.rstudio.com>

Salazar, K. A., Joffe, N. R., Dinguirard, N., Houde, P., & Castillo, M. G. (2015). Transcriptome analysis of the white body of the squid *Euprymna tasmanica* with emphasis on immune and hematopoietic gene discovery. *PloS One*, *10* (3), e0119949.

Schunter, C., Jarrold, M. D., Munday, P. L., & Ravasi, T. (2021). Diel CO<sub>2</sub> fluctuations alter the molecular response of coral reef fishes to ocean acidification conditions. *Molecular Ecology*, *30* , 5105- 5118. doi:<https://doi.org/10.1111/mec.16124>

- Schunter, C., Ravasi, T., Munday, P. L., & Nilsson, G. E. (2019). Neural effects of elevated CO<sub>2</sub> in fish may be amplified by a vicious cycle. *Conservation Physiology*, *7* (1), co2100. doi:10.1093/conphys/coz100
- Schunter, C., Welch, M. J., Nilsson, G. E., Rummer, J. L., Munday, P. L., & Ravasi, T. (2018). An interplay between plasticity and parental phenotype determines impacts of ocean acidification on a reef fish. *Nature Ecology and Evolution*, *2* (2), 334. doi:10.1038/s41559-017-0428-8
- Schunter, C., Welch, M. J., Ryu, T., Zhang, H., Berumen, M. L., Nilsson, G. E., . . . Ravasi, T. (2016). Molecular signatures of transgenerational response to ocean acidification in a species of reef fish. *Nature Climate Change*, *6*, 1014-1018. doi:10.1038/NCLIMATE3087
- Shannon, P., Markiel, A., Ozier, O., Baliga, N. S., Wang, J. T., Ramage, D., . . . Ideker, T. (2003). Cytoscape: A software environment for integrated models of biomolecular interaction networks. *Genome Research*, *13* (11), 2498-2504.
- Spady, B. L., Munday, P. L., & Watson, S.-A. (2018). Predatory strategies and behaviours in cephalopods are altered by elevated CO<sub>2</sub>. *Global Change Biology*, *24*, 2585-2596. doi:10.1111/gcb.14098
- Spady, B. L., Watson, S.-A., Chase, T. J., & Munday, P. L. (2014). Projected near-future CO<sub>2</sub> levels increase activity and alter defensive behaviours in the tropical squid *Idiosepius pygmaeus*. *Biology Open*, *3* (11), 1063-1070. doi:10.1242/bio.20149894
- Stephens, M. (2016). False discovery rates: A new deal. *Biostatistics*, *18* (2), 275-294. doi:10.1093/biostatistics/kxw041
- Strader, M. E., Wong, J. M., & Hofmann, G. E. (2020). Ocean acidification promotes broad transcriptomic responses in marine metazoans: A literature survey. *Frontiers in Zoology*, *17* (1), 7. doi:10.1186/s12983-020-0350-9
- Su, W., Rong, J., Zha, S., Yan, M., Fang, J., & Liu, G. (2018). Ocean acidification affects the cytoskeleton, lysozymes, and nitric oxide of hemocytes: A possible explanation for the hampered phagocytosis in blood clams, *Tegillarca granosa*. *Frontiers in Physiology*, *9* (619). doi:10.3389/fphys.2018.00619
- Sun, Q., Zheng, Y., Chen, X., Kong, N., Wang, Y., Zhang, Y., . . . Song, L. (2021). A diet rich in diatom improves the antibacterial capacity of Pacific oyster *Crassostrea gigas* by enhancing norepinephrine-regulated immunomodulation. *Invertebrate Survival Journal*, 56-65.
- Thomas, J., Munday, P., & Watson, S.-A. (2020). Toward a mechanistic understanding of marine invertebrate behaviour at elevated CO<sub>2</sub>. *Frontiers in Marine Science*, *7*, 345. doi:10.3389/fmars.2020.00345
- Thomas, J. T., Huerlimann, R., Schunter, C., Watson, S.-A., Munday, P. L., & Ravasi, T. (2022). *Two-toned pygmy squid (Idiosepius pygmaeus) transcriptome assembly, and transcriptomic response of the nervous system to elevated CO<sub>2</sub>* [Dataset]. doi:BioProject: PRJNA798187
- Thomas, J. T., Huerlimann, R., Schunter, C., Watson, S.-A., Munday, P. L., & Ravasi, T. (2023a). *Correlating gene expression profiles with CO<sub>2</sub> treatment and OA-affected behaviours in the two-toned pygmy squid (Idiosepius pygmaeus)* [Dataset]. doi:https://doi.org/10.25903/7dcz-th66
- Thomas, J. T., Huerlimann, R., Schunter, C., Watson, S.-A., Munday, P. L., & Ravasi, T. (2023b). *Two-toned pygmy squid (Idiosepius pygmaeus) transcriptome assembly, and transcriptomic response of the nervous system to elevated CO<sub>2</sub>* [Dataset]. doi:https://doi.org/10.25903/ha66-mm11
- Thomas, J. T., Spady, B. L., Munday, P. L., & Watson, S.-A. (2021). The role of ligand-gated chloride channels in behavioural alterations at elevated CO<sub>2</sub> in a cephalopod. *Journal of Experimental Biology*, *224* (13), jeb242335. doi:10.1242/jeb.242335
- Tomanek, L., Zuzow, M. J., Ivanina, A. V., Beniash, E., & Sokolova, I. M. (2011). Proteomic response to elevated P<sub>CO<sub>2</sub></sub> level in eastern oysters, *Crassostrea virginica*: Evidence for oxidative stress. *Journal of Experimental Biology*, *214* (11), 1836-1844. doi:10.1242/jeb.055475

- Toy, J. A., Kroeker, K. J., Logan, C. A., Takeshita, Y., Longo, G. C., & Bernardi, G. (2022). Upwelling-level acidification and pH/pCO<sub>2</sub> variability moderate effects of ocean acidification on brain gene expression in the temperate surfperch, *Embiotoca jacksoni*. *Molecular Ecology*, *31* (18), 4707-4725. doi:<https://doi.org/10.1111/mec.16611>
- Tresguerres, M., & Hamilton, T. J. (2017). Acid–base physiology, neurobiology and behaviour in relation to CO<sub>2</sub>-induced ocean acidification. *Journal of Experimental Biology*, *220* (12), 2136-2148. doi:[10.1242/jeb.144113](https://doi.org/10.1242/jeb.144113)
- Valko, M., Leibfritz, D., Moncol, J., Cronin, M. T., Mazur, M., & Telser, J. (2007). Free radicals and antioxidants in normal physiological functions and human disease. *The International Journal of Biochemistry & Cell Biology*, *39* (1), 44-84.
- Wang, J.-J., Shan, K., Liu, B.-H., Liu, C., Zhou, R.-M., Li, X.-M., . . . Yan, B. (2018). Targeting circular RNA-ZRANB1 for therapeutic intervention in retinal neurodegeneration. *Cell Death & Disease*, *9* (5), 540. doi:[10.1038/s41419-018-0597-7](https://doi.org/10.1038/s41419-018-0597-7)
- Wang, Q., Cao, R., Ning, X., You, L., Mu, C., Wang, C., . . . Zhao, J. (2016). Effects of ocean acidification on immune responses of the Pacific oyster *Crassostrea gigas*. *Fish & Shellfish Immunology*, *49*, 24-33. doi:<https://doi.org/10.1016/j.fsi.2015.12.025>
- Wang, X., Wang, M., Wang, W., Liu, Z., Xu, J., Jia, Z., . . . Wang, L. (2020). Transcriptional changes of Pacific oyster *Crassostrea gigas* reveal essential role of calcium signal pathway in response to CO<sub>2</sub>-driven acidification. *Science of The Total Environment*, *741*, 140177.
- Watson, S.-A., Lefevre, S., McCormick, M. I., Domenici, P., Nilsson, G. E., & Munday, P. L. (2014). Marine mollusc predator-escape behaviour altered by near-future carbon dioxide levels. *Proceedings of the Royal Society of London B: Biological Sciences*, *281* (1774), 20132377. doi:[10.1098/rspb.2013.2377](https://doi.org/10.1098/rspb.2013.2377)
- Williams, C. R., Dittman, A. H., McElhany, P., Busch, D. S., Maher, M. T., Bammler, T. K., . . . Gallagher, E. P. (2019). Elevated CO<sub>2</sub> impairs olfactory-mediated neural and behavioral responses and gene expression in ocean-phase coho salmon (*Oncorhynchus kisutch*). *Global Change Biology*, *25*, 963-977. doi:[10.1111/gcb.14532](https://doi.org/10.1111/gcb.14532)
- Wood, D. E., Lu, J., & Langmead, B. (2019). Improved metagenomic analysis with Kraken 2. *Genome Biology*, *20* (1), 257. doi:[10.1186/s13059-019-1891-0](https://doi.org/10.1186/s13059-019-1891-0)
- Wu, F., Lu, W., Shang, Y., Kong, H., Li, L., Sui, Y., . . . Wang, Y. (2016). Combined effects of seawater acidification and high temperature on hemocyte parameters in the thick shell mussel *Mytilus coruscus*. *Fish & Shellfish Immunology*, *56*, 554-562. doi:<https://doi.org/10.1016/j.fsi.2016.08.012>
- Xie, J., Sun, X., Li, P., Zhou, T., Jiang, R., & Wang, X. (2023). The impact of ocean acidification on the eye, cuttlebone and behaviors of juvenile cuttlefish (*Sepiella inermis*). *Marine Pollution Bulletin*, *190*, 114831. doi:<https://doi.org/10.1016/j.marpolbul.2023.114831>
- Yeh, C.-W., Kao, S.-H., Cheng, Y.-C., & Hsu, L.-S. (2013). Knockdown of cyclin-dependent kinase 10 (*cdk10*) gene impairs neural progenitor survival via modulation of *raf1a* gene expression. *Journal of Biological Chemistry*, *288* (39), 27927-27939. doi:[10.1074/jbc.M112.420265](https://doi.org/10.1074/jbc.M112.420265)
- Yu, G., Wang, L.-G., Han, Y., & He, Q.-Y. (2012). clusterProfiler: An R package for comparing biological themes among gene clusters. *OMICS: A Journal of Integrative Biology*, *16* (5), 284-287. doi:[10.1089/omi.2011.0118](https://doi.org/10.1089/omi.2011.0118)
- Zhang, T., Qu, Y., Zhang, Q., Tang, J., Cao, R., Dong, Z., . . . Zhao, J. (2021). Risks to the stability of coral reefs in the South China Sea: An integrated biomarker approach to assess the physiological responses of *Trochus niloticus* to ocean acidification and warming. *Science of The Total Environment*, *782*, 146876. doi:<https://doi.org/10.1016/j.scitotenv.2021.146876>

Zhou, Z., Wang, L., Gao, Y., Wang, M., Zhang, H., Wang, L., . . . Song, L. (2011). A monoamine oxidase from scallop *Chlamys farreri* serving as an immunomodulator in response against bacterial challenge. *Developmental & Comparative Immunology*, 35 (7), 799-807. doi:<https://doi.org/10.1016/j.dci.2011.03.014>

### Hosted file

Tables.docx available at <https://authorea.com/users/644149/articles/657150-transcriptomic-responses-in-the-nervous-system-and-correlated-behavioural-changes-of-a-cephalopod-exposed-to-ocean-acidification>

### Hosted file

Supplementary\_tables.xlsx available at <https://authorea.com/users/644149/articles/657150-transcriptomic-responses-in-the-nervous-system-and-correlated-behavioural-changes-of-a-cephalopod-exposed-to-ocean-acidification>

## Supplemental Information for:

# Transcriptomic responses in the nervous system and correlated behavioural changes of a cephalopod exposed to ocean acidification

Jodi T. Thomas, Roger Huerlimann, Celia Schunter, Sue-Ann Watson, Philip L. Munday, Timothy Ravasi

### Table of Contents:

<b>Supplementary Text S1. Water sampling methods.</b>	Page 3
<b>Supplementary Text S2. <i>de novo</i> transcriptome assembly.</b>	Page 4
<b>Supplementary Text S3. Correlating gene expression profiles with CO<sub>2</sub> treatment and OA-affected behaviours.</b>	Page 6
<b>Figure S1. Diel CO<sub>2</sub> variation at the site <i>I. pygmaeus</i> were collected.</b>	Page 8
<b>Figure S2. Detailed workflow from tissue sampling to bioinformatics analyses and statistical analyses.</b>	Page 9
<b>Figure S3. Sample dendrograms to detect sample outliers.</b>	Page 10
<b>Figure S4. Choosing and checking the soft threshold power for network construction using the CNS samples.</b>	Page 11
<b>Figure S5. Choosing and checking the soft threshold power for network construction using the eyes samples.</b>	Page 13
<b>Figure S6. Cluster dendrogram with assigned co-expression network modules before and after merging modules.</b>	Page 15
<b>Figure S7. Canonical loadings and cross loadings for each canonical function (CF) of each variable in the CNS.</b>	Page 16
<b>Figure S8. Canonical loadings and cross loadings for each canonical function (CF) of each variable in the eyes.</b>	Page 18
<b>Figure S9. Canonical correlation analysis biplot for the CNS canonical functions 1 and 2.</b>	Page 20
<b>Figure S10. Canonical correlation analysis biplot for the CNS canonical functions 1 and 3.</b>	Page 21
<b>Figure S11. Canonical correlation analysis biplot for the CNS canonical functions 2 and 3.</b>	Page 22
<b>Figure S12. Canonical correlation analysis biplot for the CNS canonical functions 1 and 4.</b>	Page 23
<b>Figure S13. Canonical correlation analysis biplot for the CNS canonical functions 2 and 4.</b>	Page 24
<b>Figure S14. Canonical correlation analysis biplot for the CNS canonical functions 3 and 4.</b>	Page 25
<b>Figure S15. Canonical correlation analysis biplot for the eyes canonical functions 1 and 2.</b>	Page 26

<b>Figure S16. Canonical correlation analysis biplot for the eyes canonical functions 1 and 3.</b>	<a href="#">Page 27</a>
<b>Figure S17. Canonical correlation analysis biplot for the eyes canonical functions 2 and 3.</b>	<a href="#">Page 28</a>
<b>Figure S18. Canonical correlation analysis biplot for the eyes canonical functions 1 and 4.</b>	<a href="#">Page 29</a>
<b>Figure S19. Canonical correlation analysis biplot for the eyes canonical functions 2 and 4.</b>	<a href="#">Page 30</a>
<b>Figure S20. Canonical correlation analysis biplot for the eyes canonical functions 3 and 4.</b>	<a href="#">Page 31</a>
<b>Figure S21. Final modules of interest in the A) CNS and B) eyes.</b>	<a href="#">Page 32</a>
<b>Figure S22. Species distribution for the top blast hits of the annotated transcriptome assembly.</b>	<a href="#">Page 33</a>
<b>Figure S23. Dotplot showing the results from gene set enrichment analysis (GSEA) using GO terms/functional categories in the CNS and eyes.</b>	<a href="#">Page 34</a>
<b>Supplementary Tables</b>	<a href="#">Page 35</a>
<b>File S1. TapeStation electropherograms for each of the 40 RNA samples used for RNA-sequencing.</b>	<a href="#">Page 38</a>
<b>References</b>	<a href="#">Page 39</a>

## Supplementary Text S1. Water sampling methods.

To evaluate the magnitude of natural diel CO<sub>2</sub> fluctuations and the ecological relevance of our experimental CO<sub>2</sub> treatment levels, water samples were taken from the same location where two-toned pygmy squid (*Idiosepius pygmaeus*) were collected. *I. pygmaeus* were collected from August - October 2019, and water samples from August - September 2021, from coastal waters around the Townsville breakwater complex. All water samples were collected with 250 mL borosilicate glass bottles. Bottles were dipped into the water upside down and at approximately 25 cm deep the bottle was inverted several times to allow water to enter and remove all air bubbles, and the lid was screwed on underwater. Each sample was taken in pairs; one was placed directly in the dark for storage until lab measurements, and the other was used immediately for measurements of water temperature (Comark C26, Norfolk, UK) and pH<sub>NBS</sub> (Seven2Go™ pro Conductivity Meter with an InLab Expert Go-ISM pH electrode, Metler Toledo). Three pairs of water samples were taken in immediate succession at each location and sampling time. All lab measurements were taken within 2.13 ± 1 hour (mean ± SD) of water sample collection. Total alkalinity was measured by Gran titration (888 Titrand, Metrohm AG, Switzerland) and salinity was measured with a conductivity sensor (HQ40d, Hach, Loveland, CO, USA). CO<sub>2</sub> values were calculated in CO<sub>2</sub>SYS v.2.1 ([https://cdiac.ess-dive.lbl.gov/ftp/co2sys/CO2SYS\\_calc\\_XLS\\_v2.1/](https://cdiac.ess-dive.lbl.gov/ftp/co2sys/CO2SYS_calc_XLS_v2.1/)) using the constants K1, K2 from Mehrbach et al. (1973) and refit by Dickson and Millero (1987) Dickson and KHSO<sub>4</sub> from Dickson et al. (2007).

To determine any spatial variation within the breakwater marina complex, three pairs of water samples were taken from each of three different locations (19°15'06.3"S 146°49'22.4"E; 19°15'08.1"S 146°49'27.6"E; 19°15'11.8"S 146°49'21.6"E), both before first light (approximately 5:30) and mid-afternoon (approximately 13:30). CO<sub>2</sub> levels were consistent across these three locations, therefore all subsequent sampling was done from one location (19°15'06.3"S 146°49'22.4"E). To determine the best time for afternoon sampling to capture maximum change in CO<sub>2</sub> levels, three pairs of water samples were collected at each of three time points; 12:30, 13:30 and 14:30. These time points were chosen based on previous research that found minimum CO<sub>2</sub> was reached between 12:30 and 14:20 at Lizard Island, Great Barrier Reef (Hannan et al., 2020). CO<sub>2</sub> levels were consistent across these three time points, therefore all subsequent sampling was done at 13:30. After these initial checks were completed, water sampling was carried out to determine any diel CO<sub>2</sub> variation. Three pairs of water samples were taken before first light (approximately 5:00) and at 13:30 across five days of differing tidal heights, all from the same location. Figure S1 shows the diel CO<sub>2</sub> variation. All raw data from water sampling can be found at DOI 10.25903/ha66-mm11 (this DOI is embargoed until peer-reviewed publication).

## **Supplementary Text S2. *de novo* transcriptome assembly**

### ***ISO-sequencing***

Library preparation and sequencing was carried out by the Sequencing Section, Okinawa Institute of Science and Technology Graduate University, Japan on four samples that were also used for RNA-seq, one of each tissue type and CO<sub>2</sub> level. RNA from the eyes was purified with oligo d(T) beads due to carry over of pigmentation (NEBNext® Poly(A) mRNA Magnetic Isolation Module, New England Biolabs Inc.). RNA was quantified by Qubit 4 Fluorometer (Qubit RNA HS Assay Kit, Life Technologies). One library was prepared for each sample following the ISO-Seq™ Express Template Preparation for Sequel® and Sequel II Systems protocol with standard size selection (86 µL ProNex® Beads). Libraries were sequenced on one SMRTcell of a PacBio Sequel II.

### ***De novo transcriptome assembly***

The ISO-seq data was processed using the PacBio isoseq3 pipeline. The raw subreads were compiled into circular consensus sequence (ccs) reads by ccs (v4.2.0) with the minimum number of full passes set at three and the minimum predicted accuracy of a read at 0.9. Lima (v1.11.0) was used to classify the ccs reads as full-length (FL) (by the presence of both 5' and 3' primers) and remove index sequences with '--peek-guess'. The resulting FL reads from each tissue/barcode were combined and isoseq3 refine (v3.3.0) was used to remove concatemers and polyA tails, producing full-length non-concatemer (FLNC) reads. The FLNC reads were then clustered by isoform using isoseq3 cluster (v3.3.0), using the ccs quality values ('--use-qvs') to obtain a consensus sequence for each isoform. Redundancy removal was performed using CD-HIT-EST (v4.6) (Fu et al., 2012; Li and Godzik, 2006) to collapse contigs with at least 99% identity. TransDecoder (v5.5.0) (Brian and Papanicolaou, n.d.) was used to identify candidate coding regions/open reading frames (ORFs). The single best ORF per contig was chosen based on blast homology to known proteins in the NCBI nr database subset for mollusca (nr\_mollusca, downloaded 01/2021) using BLASTp from BLAST+ (v2.10.0+) with max\_target\_seqs 1 and an e-value cut-off of 1<sup>-5</sup>, and then based on ORF length (minimum 100 amino acids). The entire transcript was retained for each identified ORF.

The quality and completeness of the transcriptome was assessed before and after redundancy removal, and for the final transcriptome assembly (after ORF identification by TransDecoder). Quality was assessed using Transrate (v1.0.3) (Smith-Unna et al., 2016) and completeness using Benchmarking Universal Single-Copy Orthologs (BUSCO v4.1.2) (Manni et al., 2021), using the lineage mollusca\_odb10.2019-11-20. Quality and completeness were also assessed by blasting the transcriptome against nr\_mollusca (e-value cut-off = 1<sup>-5</sup>, '-max\_target\_seqs 1', BLASTx from BLAST+ (v2.10.0+) (Camacho et al., 2009)), and mapping the trimmed, decontaminated RNA-seq reads to the transcriptome assembly (local alignment, Bowtie2 (v2.4.1) (Langmead and Salzberg, 2012)).

### ***Transcriptome annotation***

The transcriptome was blasted against the entire NCBI nr database (downloaded 01/2021) using BLASTx from BLAST+ (v2.10.0+) (Camacho et al., 2009) with an e-value cut-off of  $1^{-5}$ , outfmt 14, and '-num-alignments' and '-max\_hsp' both set at 20. Functional annotation was carried out in OmicsBox (v1.4.12) (BioBam Bioinformatics, 2019) using BLAST2GO mapping (Goa version 2020.10, all default settings) (Götz et al., 2008), followed by BLAST2GO annotation (all default settings) (Götz et al., 2008) and InterProScan (v5.50-84.0, all default settings) (Jones et al., 2014). The InterProScan GOs were then merged with the annotations.

## **Supplementary Text S3. Correlating gene expression profiles with CO<sub>2</sub> treatment and OA-affected behaviours.**

### ***Gene co-expression network construction and module detection***

To analyse the correlation between gene expression and behavioural traits of squid across CO<sub>2</sub> treatments, we employed weighted gene co-expression network analysis (WGCNA) followed by canonical correlation analysis (CCA) on the CNS and eyes, separately (Figure 1). The gene-level counts for all 20 samples from each tissue were normalised, transcripts with low read counts were removed ( $\leq 10$  counts in  $\geq 90\%$  samples) and the remaining count data was variance stabilised in DESeq2 (v1.30.1) (Love et al., 2014). This count data was then used in the WGCNA package (v1.70-3) (Langfelder and Horvath, 2008) for co-expression network construction and module detection. No genes were identified as outliers, using 'goodSamplesGenes'. To detect any outliers among the samples themselves, a sample dendrogram was created using hierarchical clustering with the 'average' method. Three and two obvious sample outliers were identified and removed from the analysis in the CNS and eyes, respectively (Figure S3). Soft thresholding power was evaluated and powers of 14 and 13 were chosen for the CNS and eyes, respectively, to approximate a scale free topology (Figures S4 and S5). The following co-expression network construction and module detection steps were carried out on a high-performance computing cluster at Okinawa Institute of Science and Technology, Japan to allow multiple threads for a full network analysis occurring in one block. A signed correlation network adjacency was calculated using Pearson correlation and the chosen soft thresholding power. The adjacency was transformed into a signed topological overlap matrix (TOM) and the corresponding dissimilarity was calculated (1-TOM). A cluster dendrogram of genes was created using hierarchical clustering with the 'average' method and the dissimilarity TOM. Modules were detected using dynamic tree cut with the hybrid method, a minimum cluster size of 30, an intermediate sensitivity to cluster splitting (deepSplit = 2) and the Partitioning Around Medoids (PAM)-like step set to not respect the dendrogram (pamRespectsDendro = FALSE). Modules with a correlation of  $\geq 0.70$  were then merged (Figure S6, Tables S1 and S2). Eigengenes were calculated for each final module, which is the first principal component in the corresponding module used to represent the gene expression profiles of that module. These module eigengenes (MEs) allow gene modules to be correlated with external traits (Langfelder and Horvath, 2008).

### ***Module eigengene correlation with behavioural traits***

Canonical correlation analysis (CCA) using package CCA (v1.2.1) (González et al., 2008) was used to explore the correlations between the two sets of variables from the same individual squid: ME set = MEs from each module; traits set = CO<sub>2</sub> level (current-day or elevated) and behavioural traits (active time (s), distance (cm), speed (cm/s), time in Zone A (s), whether the squid displayed an exploratory/aggressive interaction (yes/no), number of exploratory/aggressive interactions). The canonical loadings and cross-loadings were calculated for the first four canonical functions (CF) in the CNS and eyes, separately. The first four CFs were chosen for interpretation as they explained a substantial amount of variance between the traits set and MEs set (canonical correlation  $> 0.6$ ) (Sherry and Henson, 2005). Heatmaps of all canonical loadings and cross-loadings for all variables of each set were created for each of the four CFs (Figures S7 and S8). If

the canonical loading and cross-loading of a given variable from both the ME set and traits set were  $\geq 0.3$  for the same CF, this ME and trait were considered correlated. A cut-off value of 0.3 is commonly used (Kabir et al., 2014; Lambert and Durand, 1975) and was a clear cut-off for this dataset (Figures S7 and S8). Biplots were created for each two-way combination of the four CFs (Figures S9 – S20). MEs and traits within the same or opposite quarters of the biplot, and sitting on or outside the biplot inner ring with a radius of 0.5, were considered positively or negatively correlated, respectively. If MEs and traits were considered correlated by both the canonical loadings/cross-loadings heatmap and biplots they were identified as modules of interest for the given trait(s).

### ***Module membership vs gene significance***

The Pearson correlation of module membership (MM, higher value indicates the gene is more highly connected to the given module) and gene significance (GS, higher value indicates a more biologically relevant gene) was used to check the modules of interest identified by CCA (Langfelder and Horvath, 2008). A correlation of GS and MM imply that genes more highly connected with a given module also tend to be more highly correlated with the given trait, providing another measure for the importance of this module with the given trait (Langfelder and Horvath, 2008). All modules of interest initially identified by CCA that had a MM vs GS correlation (R-value)  $> 0.2$ , a commonly used threshold for evidence of a weak correlation (Evans, 1996), were chosen as the final modules of interest (Figure S21).

### ***Identification of hub genes***

Within the final modules of interest, the MM and GS values of each gene were used as a screening method to identify biologically relevant, highly interconnected hub genes (Fuller et al., 2007; Horvath and Dong, 2008; Langfelder and Horvath, 2008), i.e. to find genes correlated with CO<sub>2</sub> treatment and each behavioural trait. Hub genes were defined as those genes within the final modules of interest with a very strong correlation with the module (MM  $> 0.8$ ) and a moderate correlation with the given trait (GS  $> 0.4$ ). As a final check of these identified hub genes, the Pearson correlation (R-value) between the normalised expression of each hub gene and the given trait was calculated and genes with a very weak correlation (R  $< 0.2$ ) were excluded. This resulted in the final list of hub genes. All hub genes for CO<sub>2</sub> treatment were compared across tissues to identify hub genes for CO<sub>2</sub> treatment that are CNS-specific, eyes-specific or found in both tissues. Hub genes for CO<sub>2</sub> treatment that were also a hub gene for one or more behavioural traits were identified as genes correlated with the associated OA-induced behavioural change.

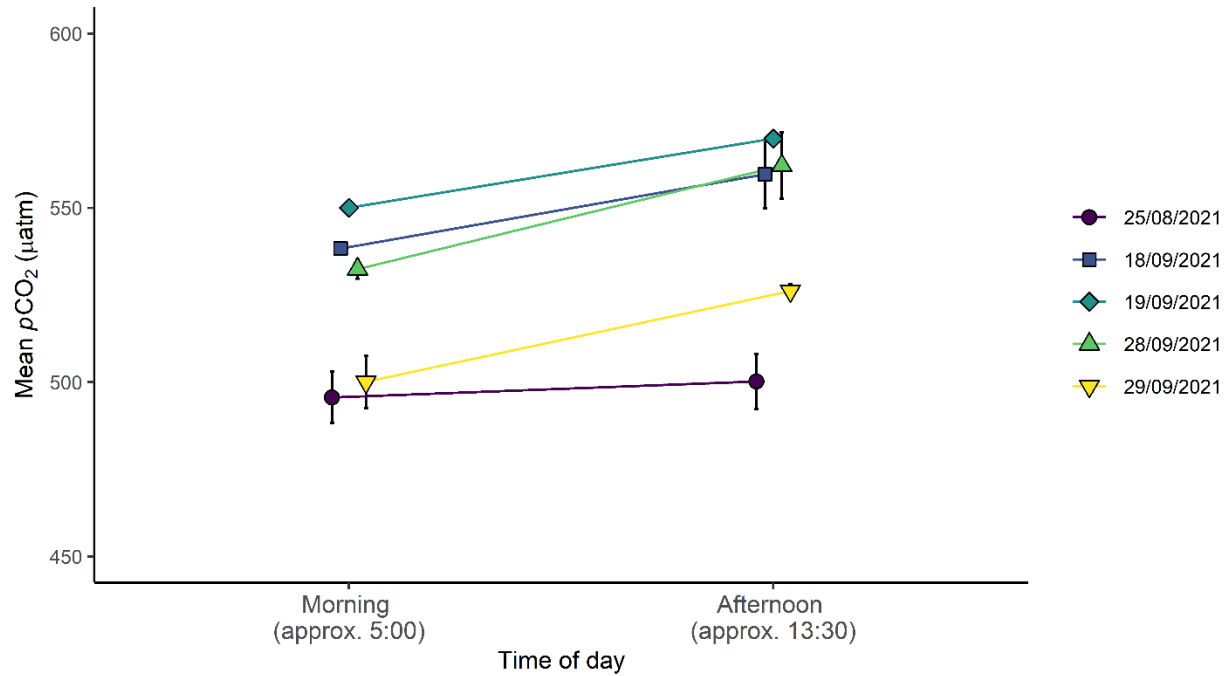


**Figure S1. Diel CO<sub>2</sub> variation at the site *I. pygmaeus* were collected.** Water samples were taken to measure CO<sub>2</sub> levels before first light at approximately 5:00 (morning) and at approximately 13:30 (afternoon) across five days. Points represent the mean ± standard deviation.

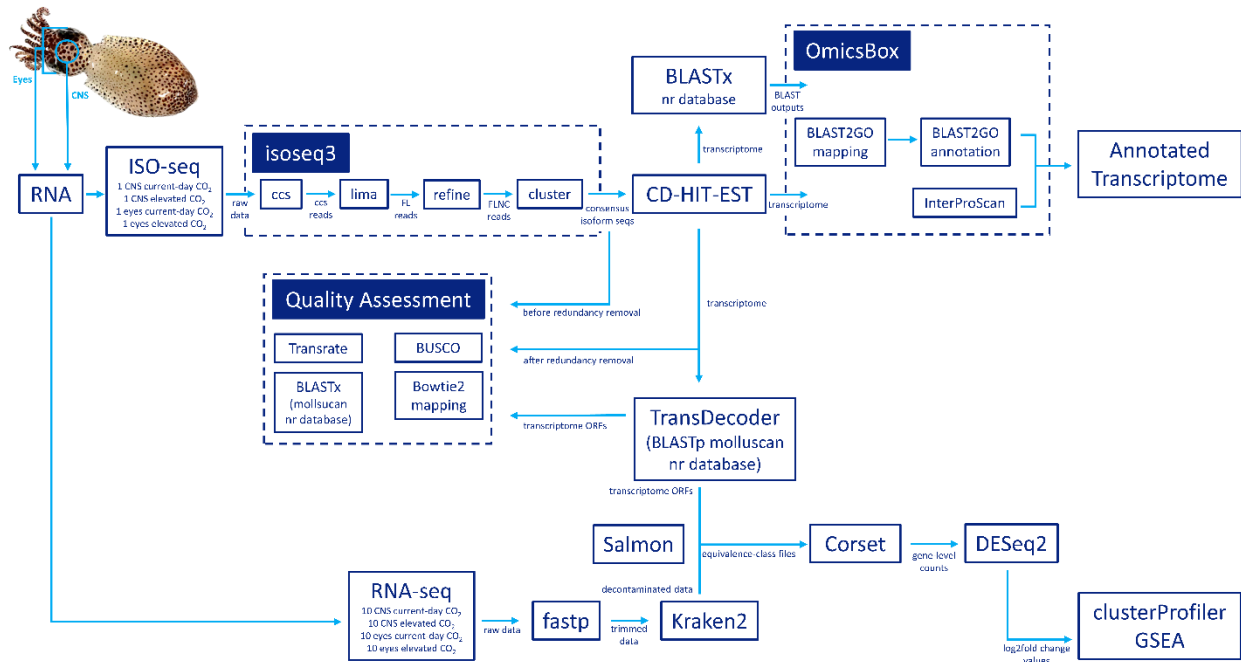


**Figure S2. Detailed workflow from tissue sampling to bioinformatics analyses and statistical analyses.** ccs = circular consensus sequence, DE = differentially expressed, FL = full length, FLNC = full-length non-concatemer, GSEA = gene set enrichment analysis, ISO-seq = PacBio long read ISO-sequencing, ORF = open reading frame, RNA-seq = RNA sequencing, seqs = sequences.

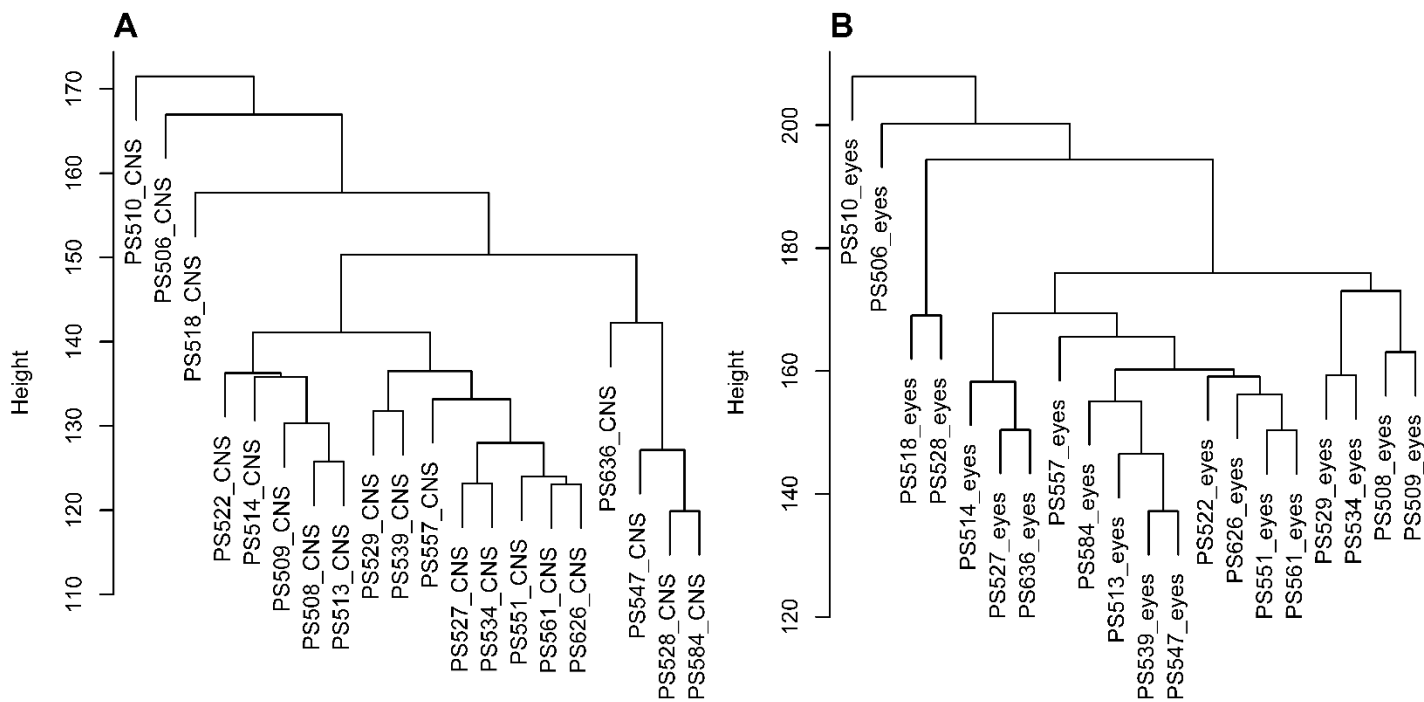


**Figure S3. Sample dendrograms to detect sample outliers.** Created using hierarchical clustering with the 'average' method. Three and two outliers were detected in the A) CNS and B) eyes, respectively. PS510\_CNS, PS506\_CNS, PS518\_CNS, PS510\_eyes and PS506\_eyes were removed as they were sample outliers.

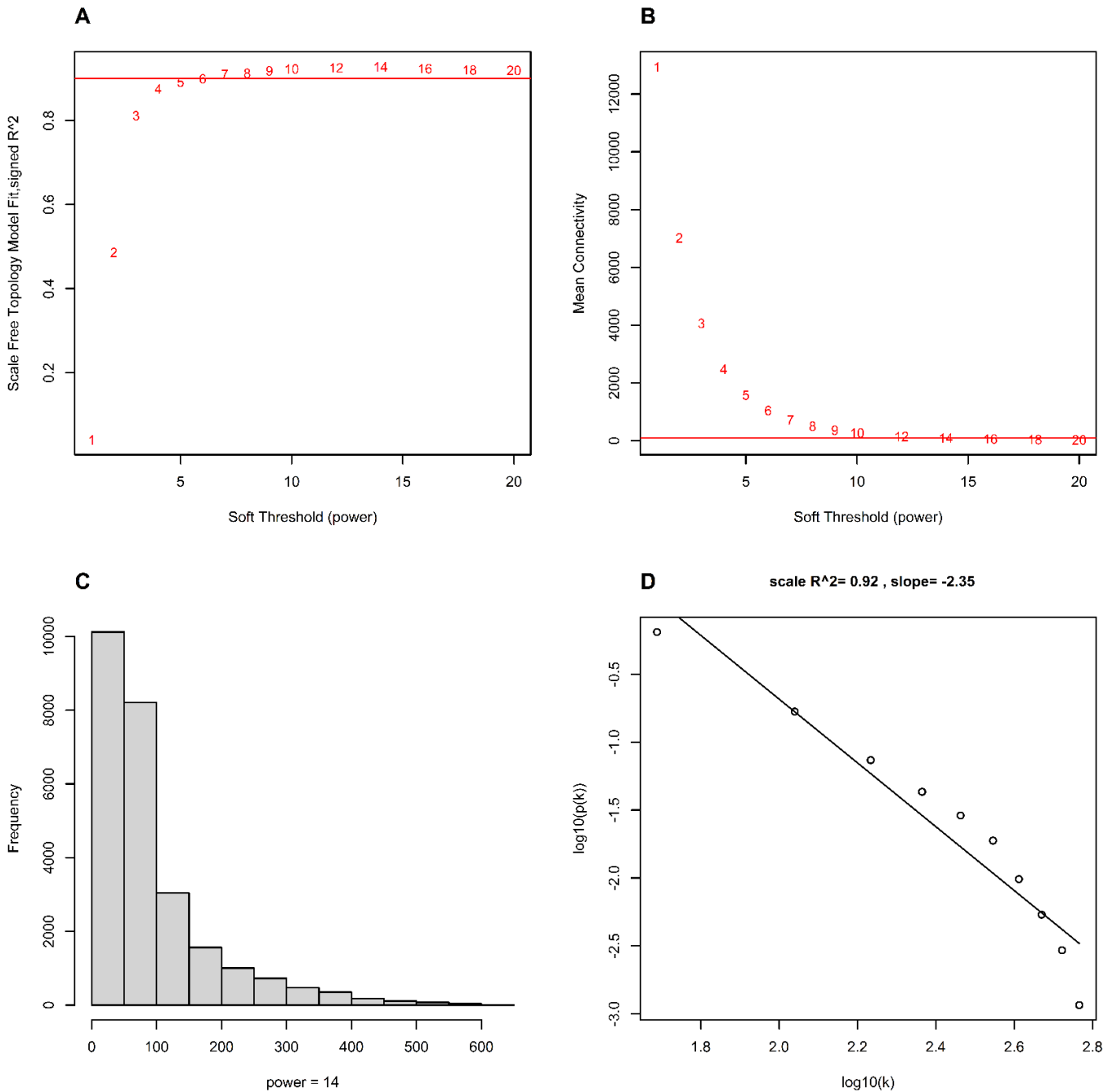


**Figure S4. Choosing and checking the soft threshold power for network construction using the CNS samples.** A) Scale-free topology fit index as a function of the soft-threshold power shows the network reaches approximately a scale free topology ( $R^2 > 0.9$ ) when the soft threshold power is 7, however B) mean connectivity as a function of the soft threshold power shows mean connectivity remains high and mean connectivity only drops below 100 at a soft threshold power of 14. C) and D) were used to check the chosen soft threshold power of 14 approximates a scale free topology.

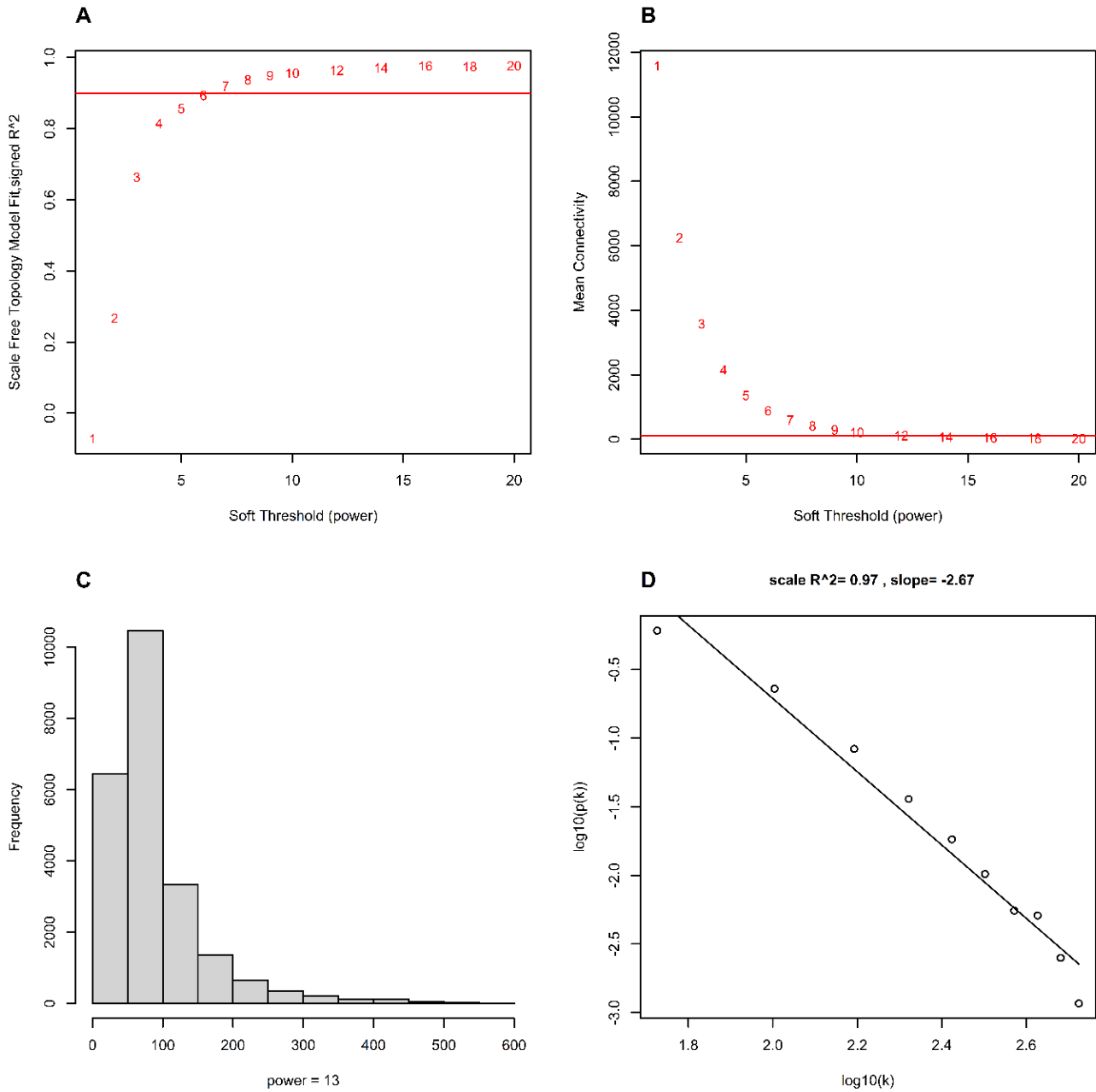


**Figure S5. Choosing and checking the soft threshold power for network construction using the eyes samples.** A) Scale-free topology fit index as a function of the soft-threshold power shows the network reaches approximately a scale free topology ( $R^2 > 0.9$ ) when the soft threshold power is 7, however B) mean connectivity as a function of the soft threshold power shows mean connectivity remains high and mean connectivity only drops below 100 at a soft threshold power of 13. C) and D) were used to check the chosen soft threshold power of 13 approximates a scale free topology.

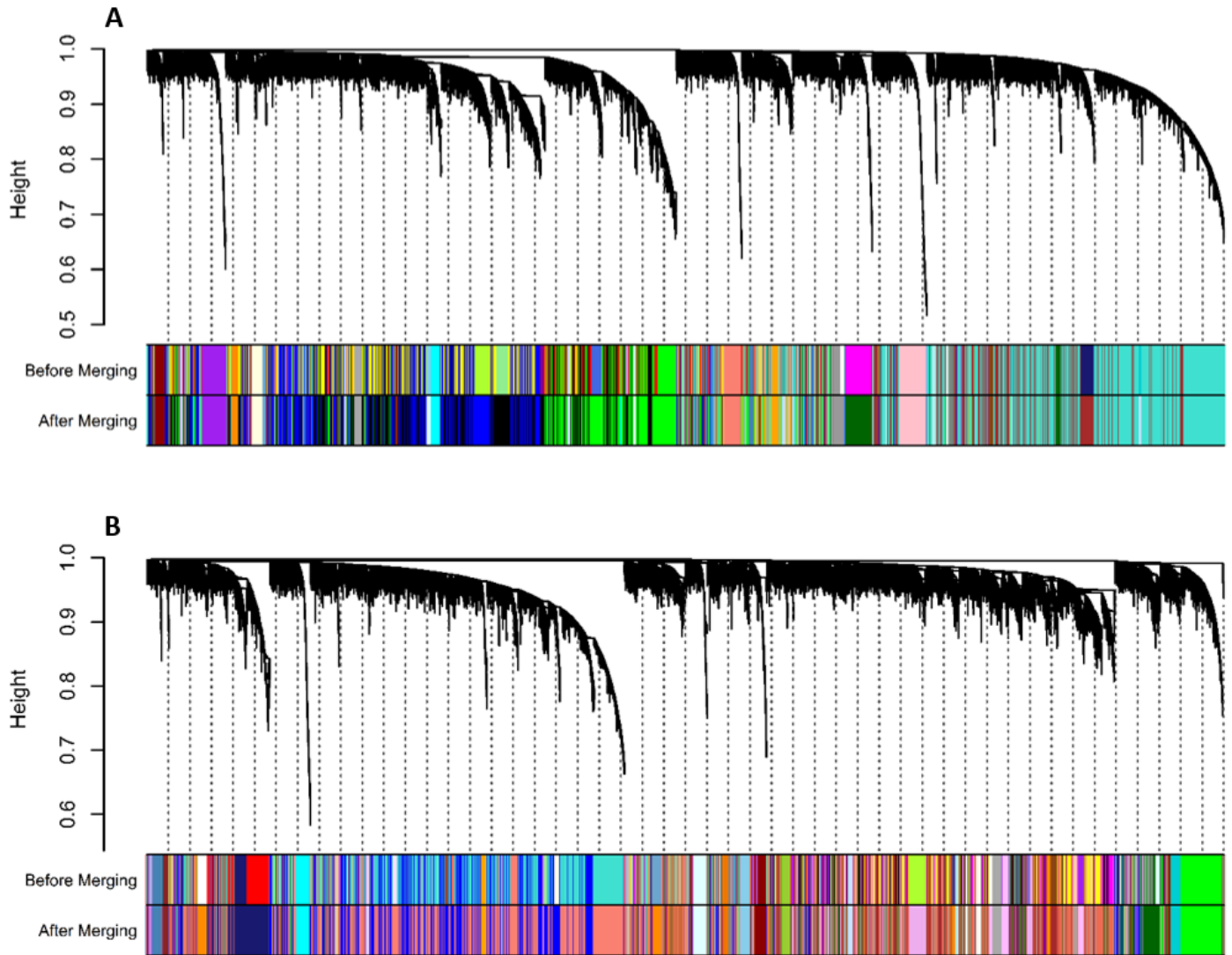


**Figure S6. Cluster dendrogram with assigned co-expression network modules before and after merging modules.** In the A) CNS and B) eyes. Each line in the cluster dendrogram is a gene and each module is represented by a different colour.

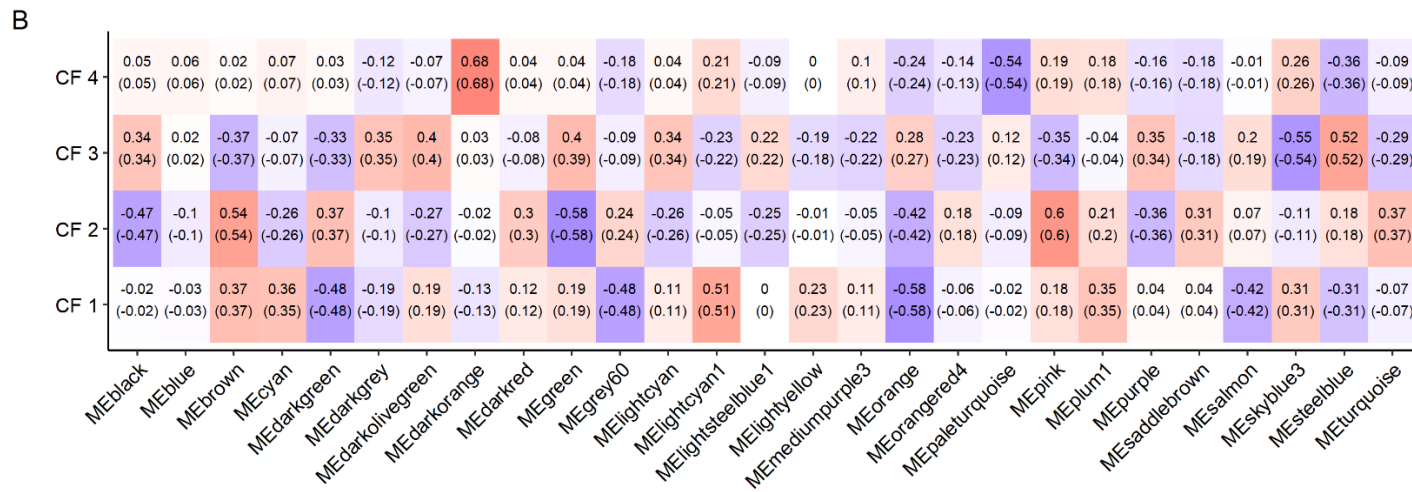
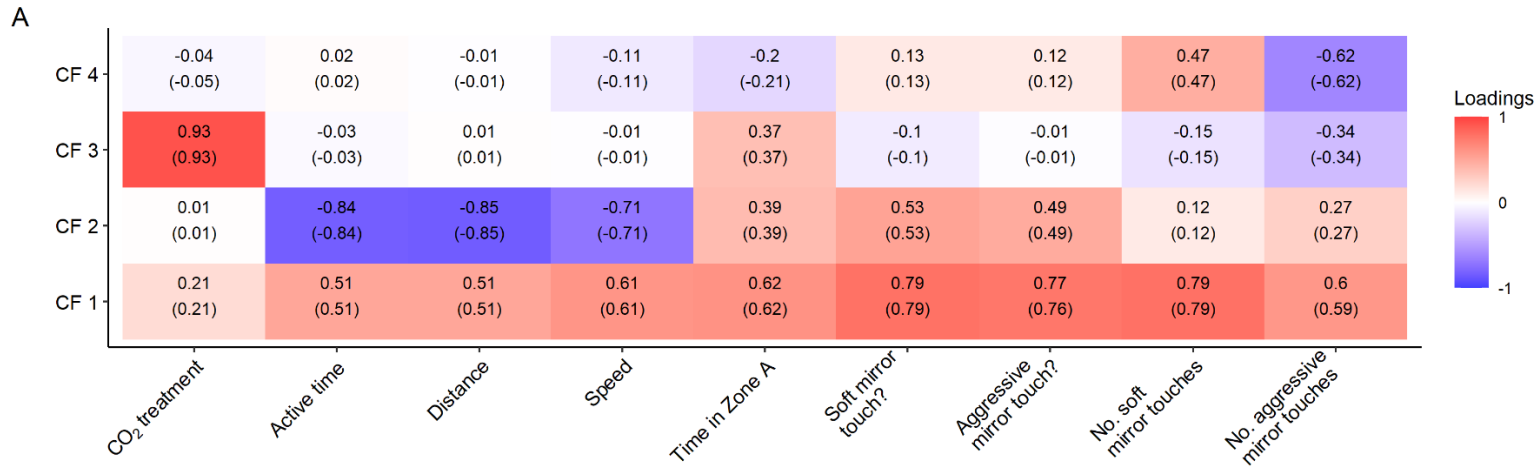
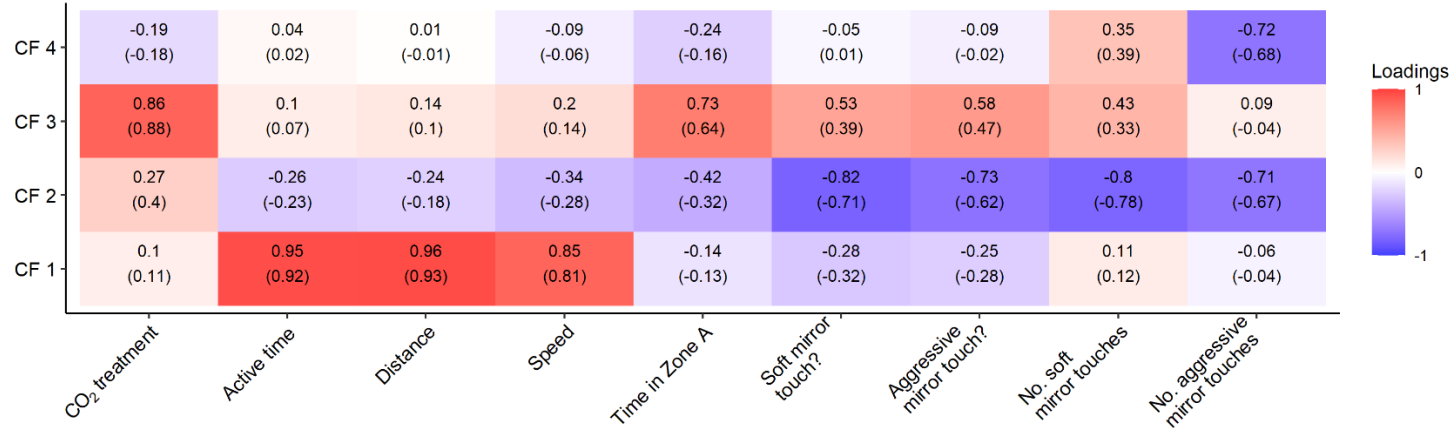


**Figure S7. Canonical loadings and cross loadings for each canonical function (CF) of each variable in the CNS.** In the A) traits set and B) module eigengenes (MEs) set. Canonical loadings are shown above canonical cross-loadings, which are in brackets. Colouration depicts canonical loadings.

A



B

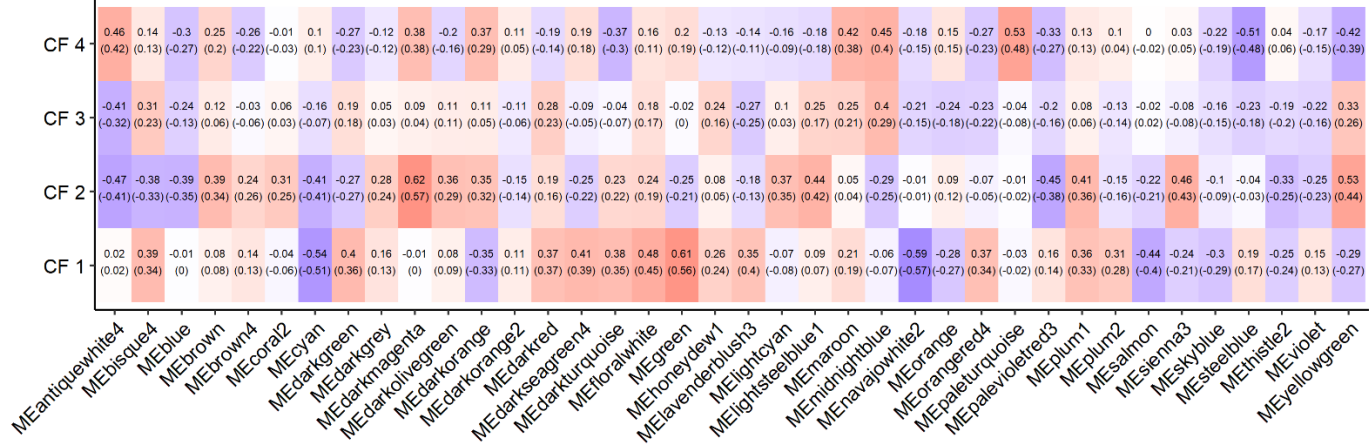


**Figure S8. Canonical loadings and cross loadings for each canonical function (CF) of each variable in the eyes.** In the A) traits set and B) module eigengenes (MEs) set. Canonical loadings are shown above canonical cross-loadings, which are in brackets. Colouration depicts canonical loadings.

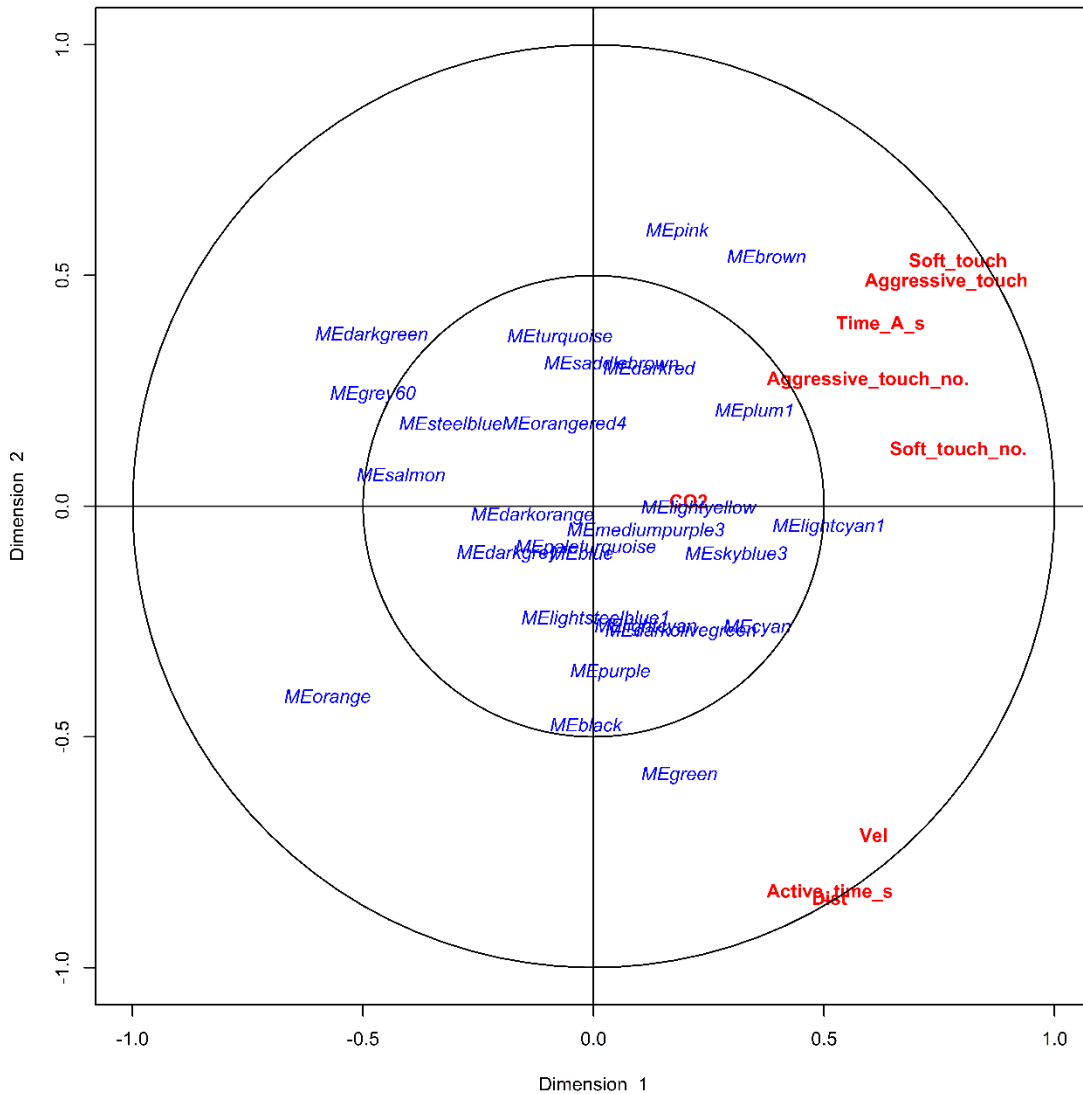


**Figure S9. Canonical correlation analysis biplot for the CNS canonical functions 1 and 2.** Depicting where the module eigengenes (MEs) lie in space in relation to the traits for the CNS, for canonical functions (dimensions) 1 and 2. Variables from the MEs set and the traits set are in blue and red, respectively. The inner ring is set at a radius of 0.5.

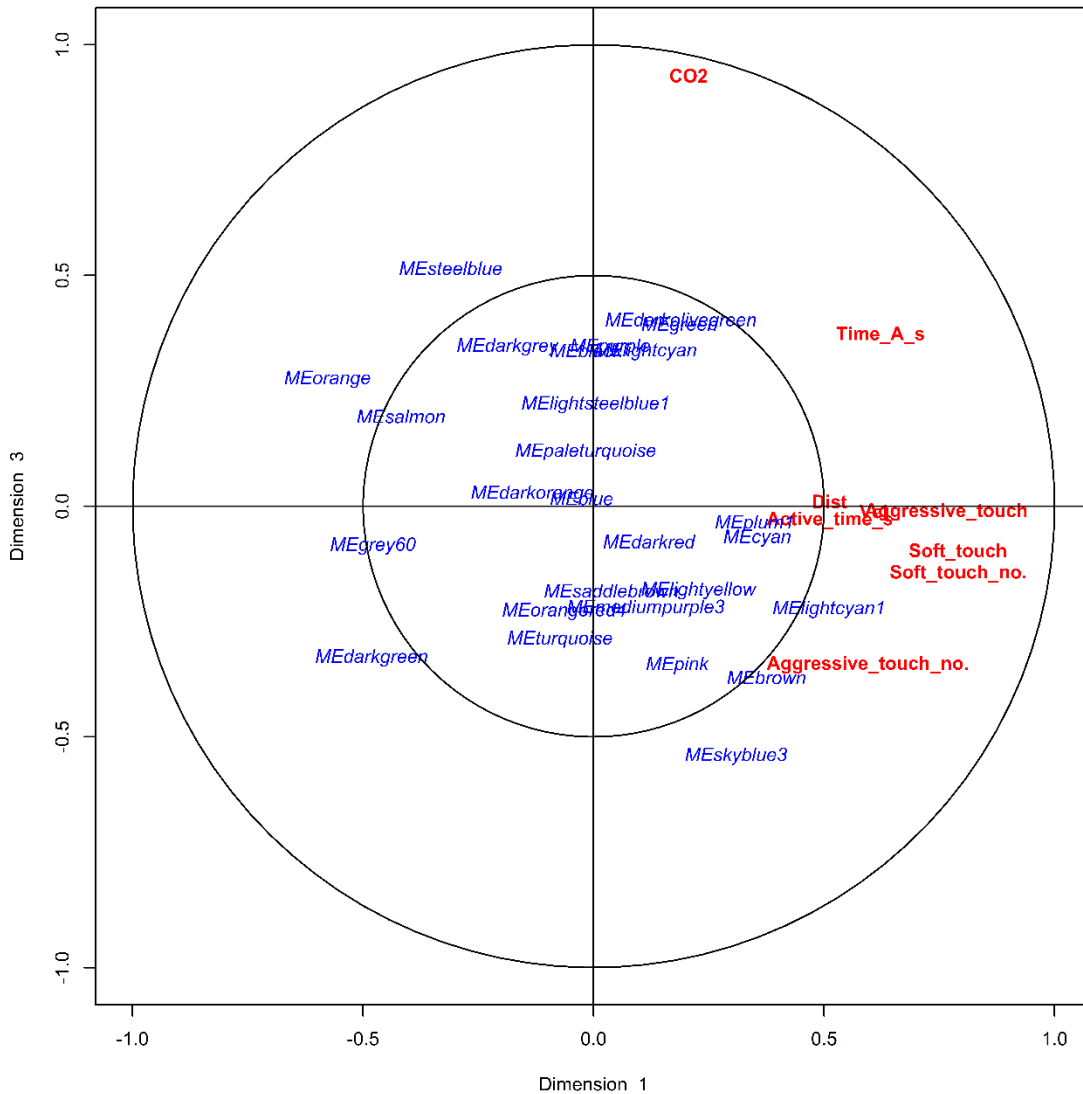


**Figure S10. Canonical correlation analysis biplot for the CNS canonical functions 1 and 3.** Depicting where the module eigengenes (MEs) lie in space in relation to the traits for the CNS, for canonical functions (dimensions) 1 and 3. Variables from the MEs set and the traits set are in blue and red, respectively. The inner ring is set at a radius of 0.5.

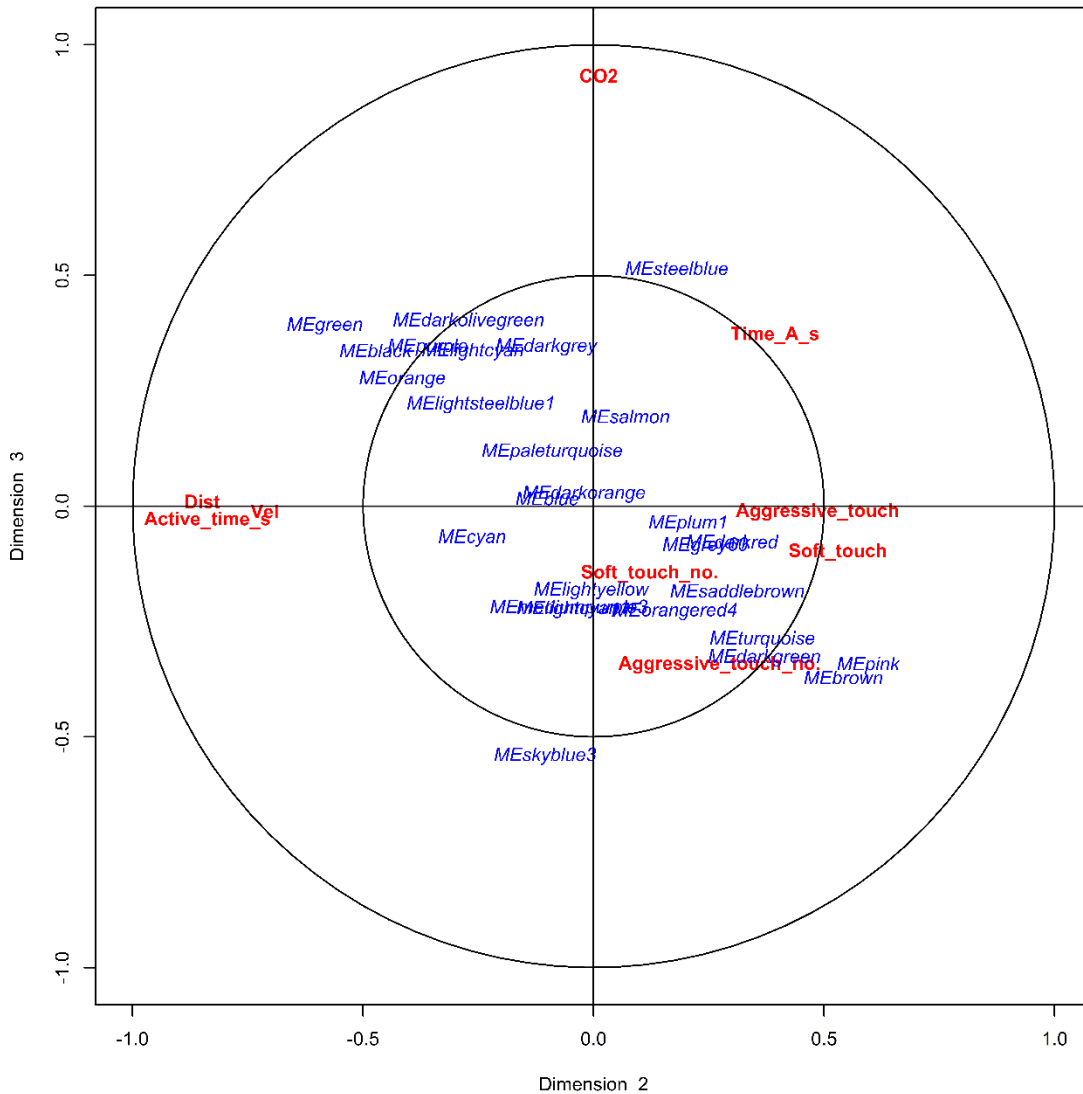


**Figure S11. Canonical correlation analysis biplot for the CNS canonical functions 2 and 3.** Depicting where the module eigengenes (MEs) lie in space in relation to the traits for the CNS, for canonical functions (dimensions) 2 and 3. Variables from the MEs set and the traits set are in blue and red, respectively. The inner ring is set at a radius of 0.5.

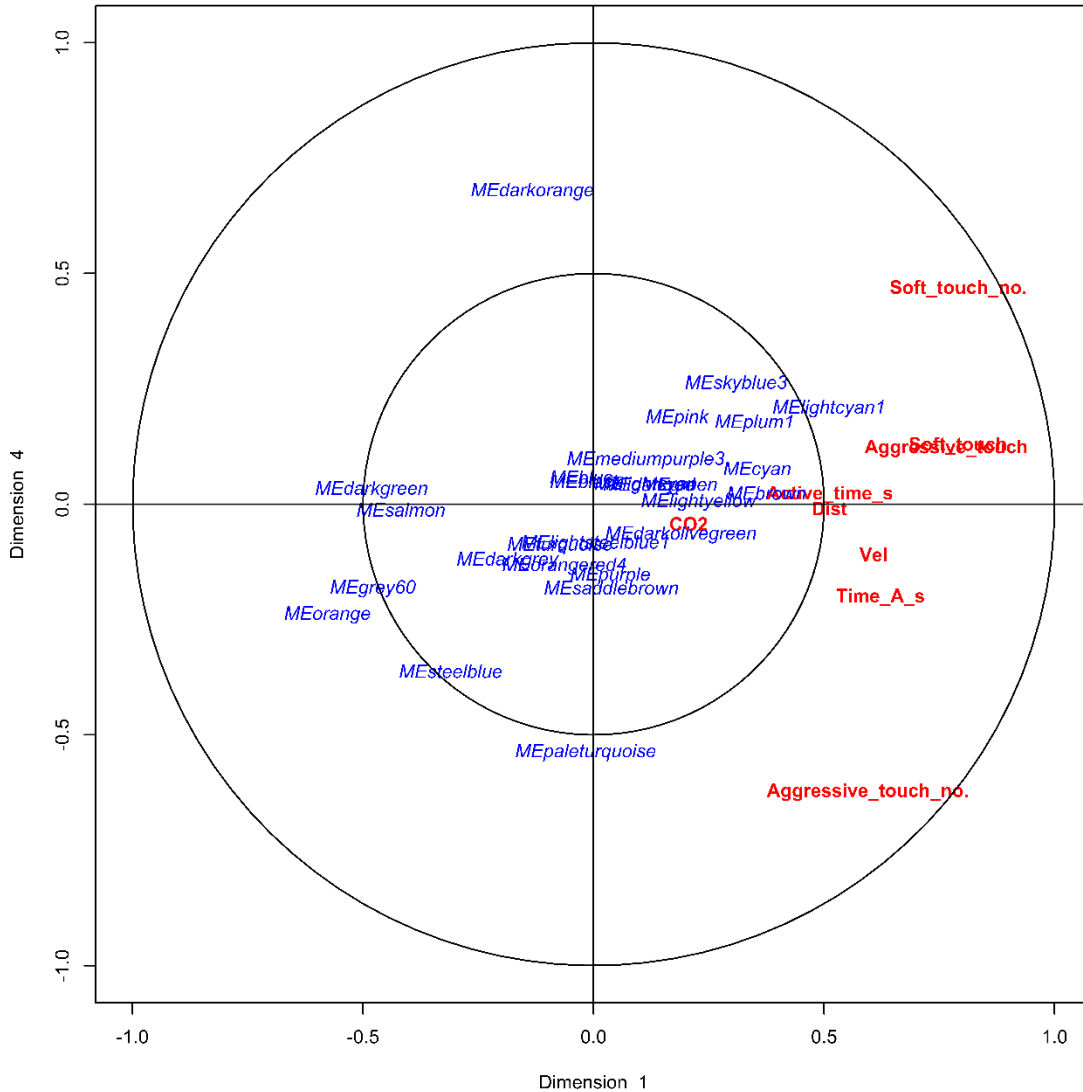


**Figure S12. Canonical correlation analysis biplot for the CNS canonical functions 1 and 4.** Depicting where the module eigengenes (MEs) lie in space in relation to the traits for the CNS, for canonical functions (dimensions) 1 and 4. Variables from the MEs set and the traits set are in blue and red, respectively. The inner ring is set at a radius of 0.5.

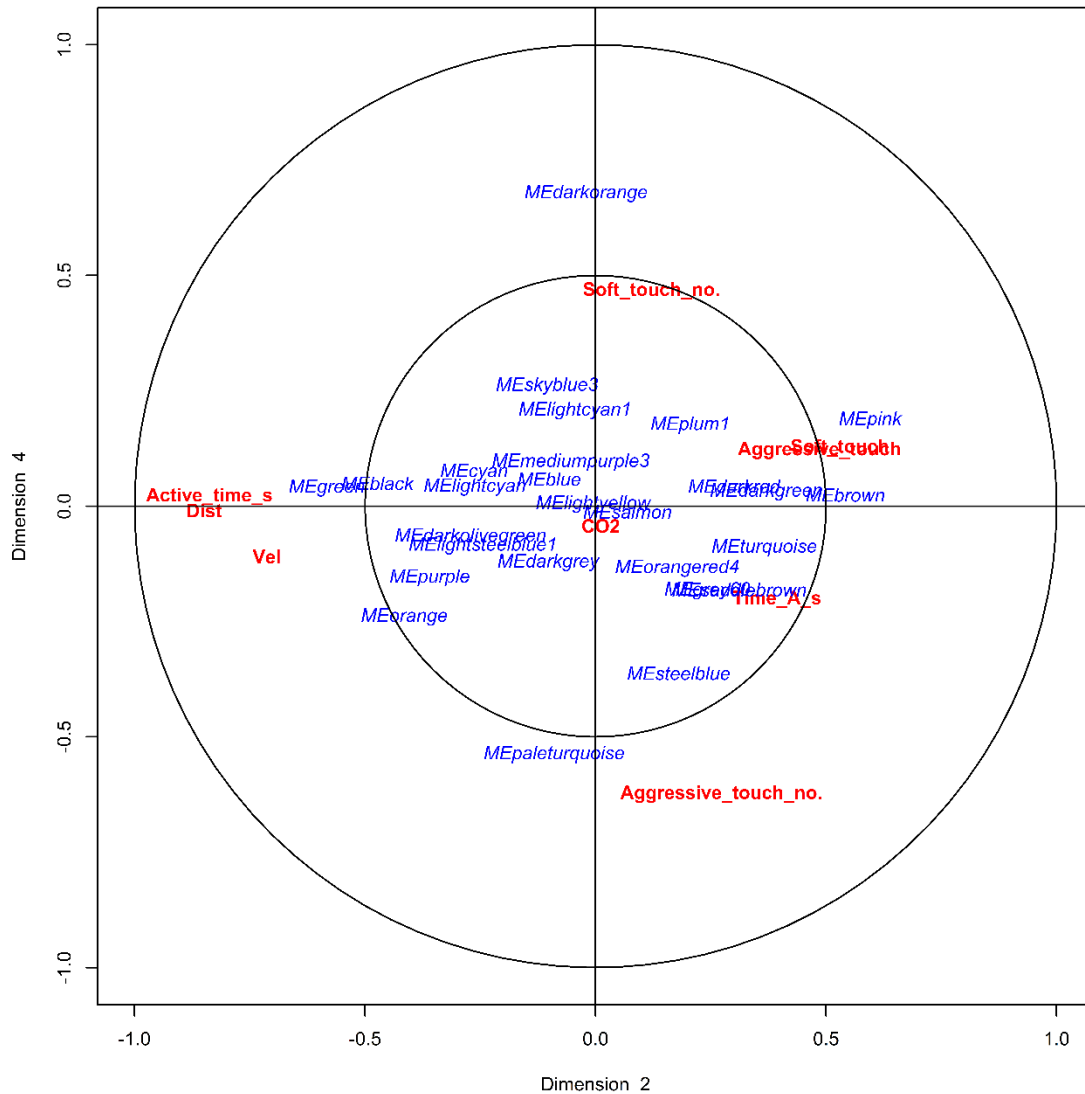


**Figure S13. Canonical correlation analysis biplot for the CNS canonical functions 2 and 4.** Depicting where the module eigengenes (MEs) lie in space in relation to the traits for the CNS, for canonical functions (dimensions) 2 and 4. Variables from the MEs set and the traits set are in blue and red, respectively. The inner ring is set at a radius of 0.5.

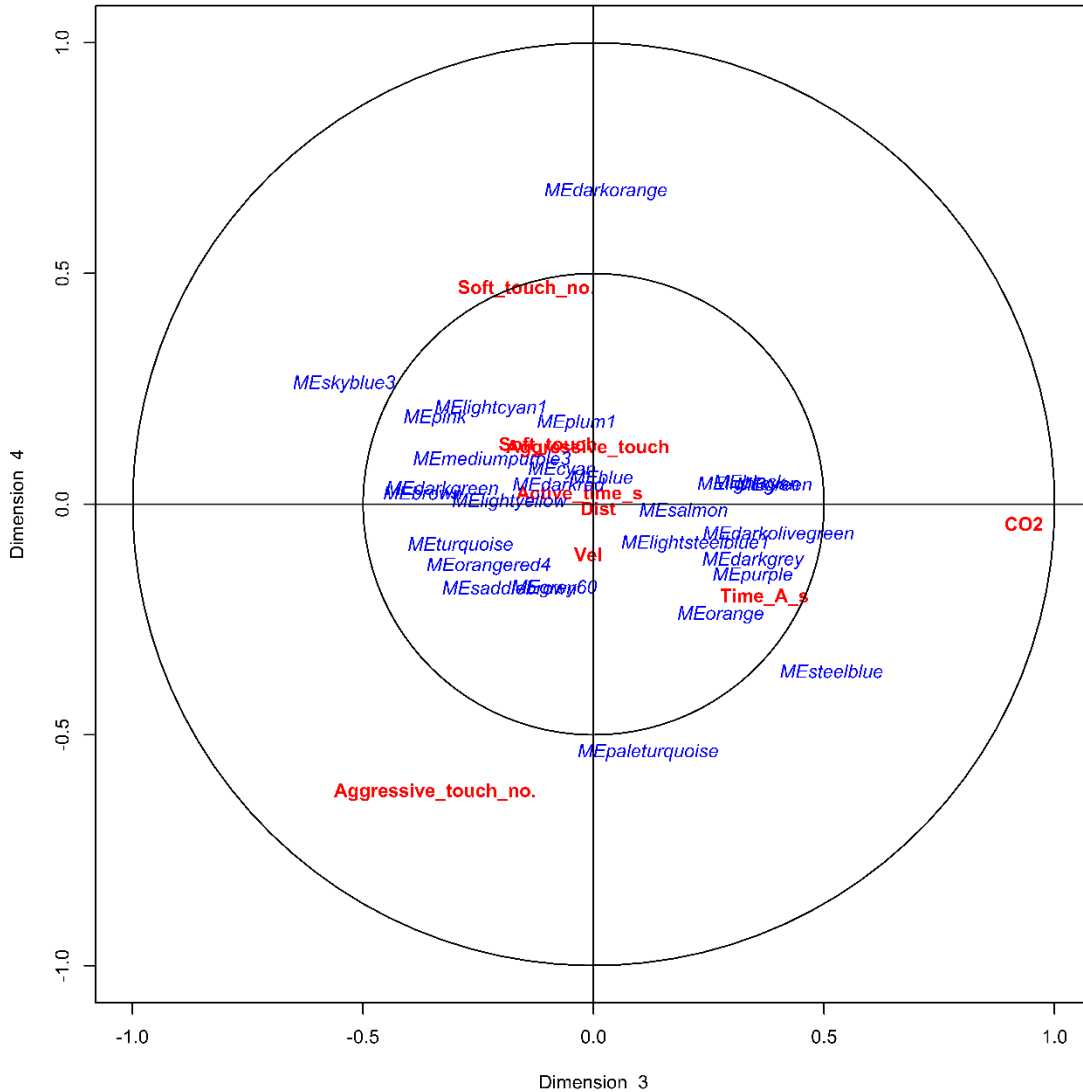


**Figure S14. Canonical correlation analysis biplot for the CNS canonical functions 3 and 4.** Depicting where the module eigengenes (MEs) lie in space in relation to the traits for the CNS, for canonical functions (dimensions) 3 and 4. Variables from the MEs set and the traits set are in blue and red, respectively. The inner ring is set at a radius of 0.5.

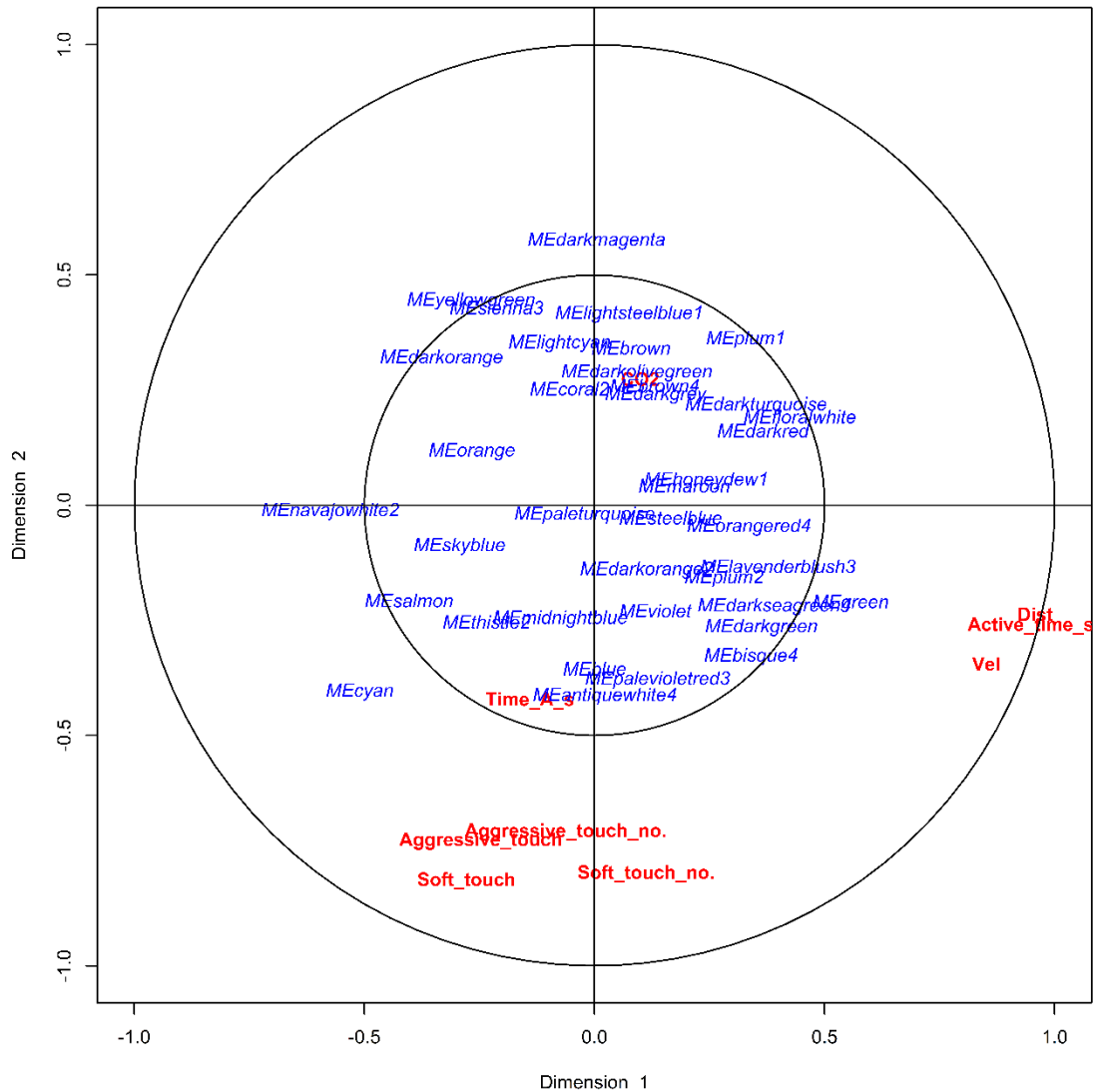


**Figure S15. Canonical correlation analysis biplot for the eyes canonical functions 1 and 2.** Depicting where the module eigengenes (MEs) lie in space in relation to the traits for the eyes, for canonical functions (dimensions) 1 and 2. Variables from the MEs set and the traits set are in blue and red, respectively. The inner ring is set at a radius of 0.5.

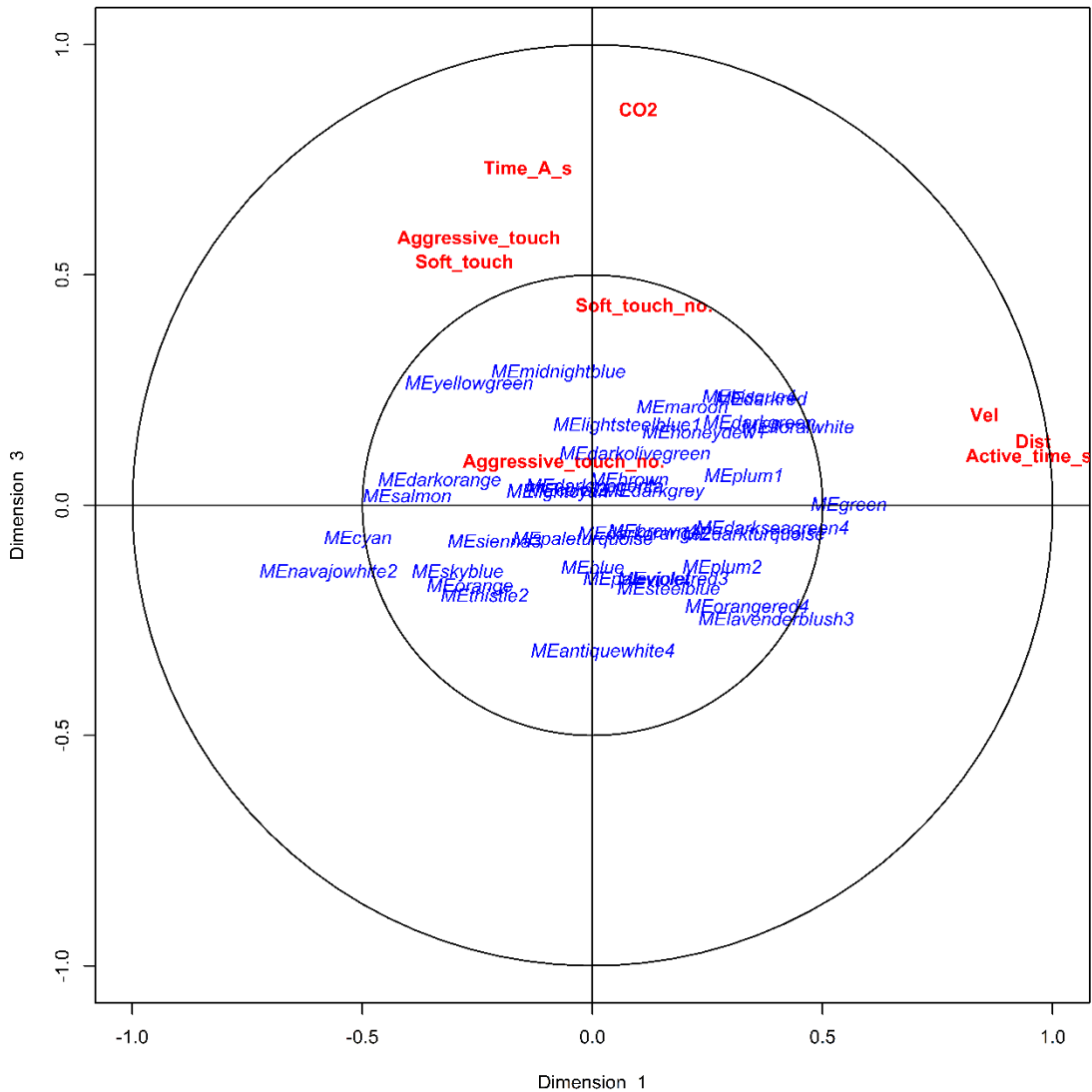


**Figure S16. Canonical correlation analysis biplot for the eyes canonical functions 1 and 3.** Depicting where the module eigengenes (MEs) lie in space in relation to the traits for the eyes, for canonical functions (dimensions) 1 and 3. Variables from the MEs set and the traits set are in blue and red, respectively. The inner ring is set at a radius of 0.5.



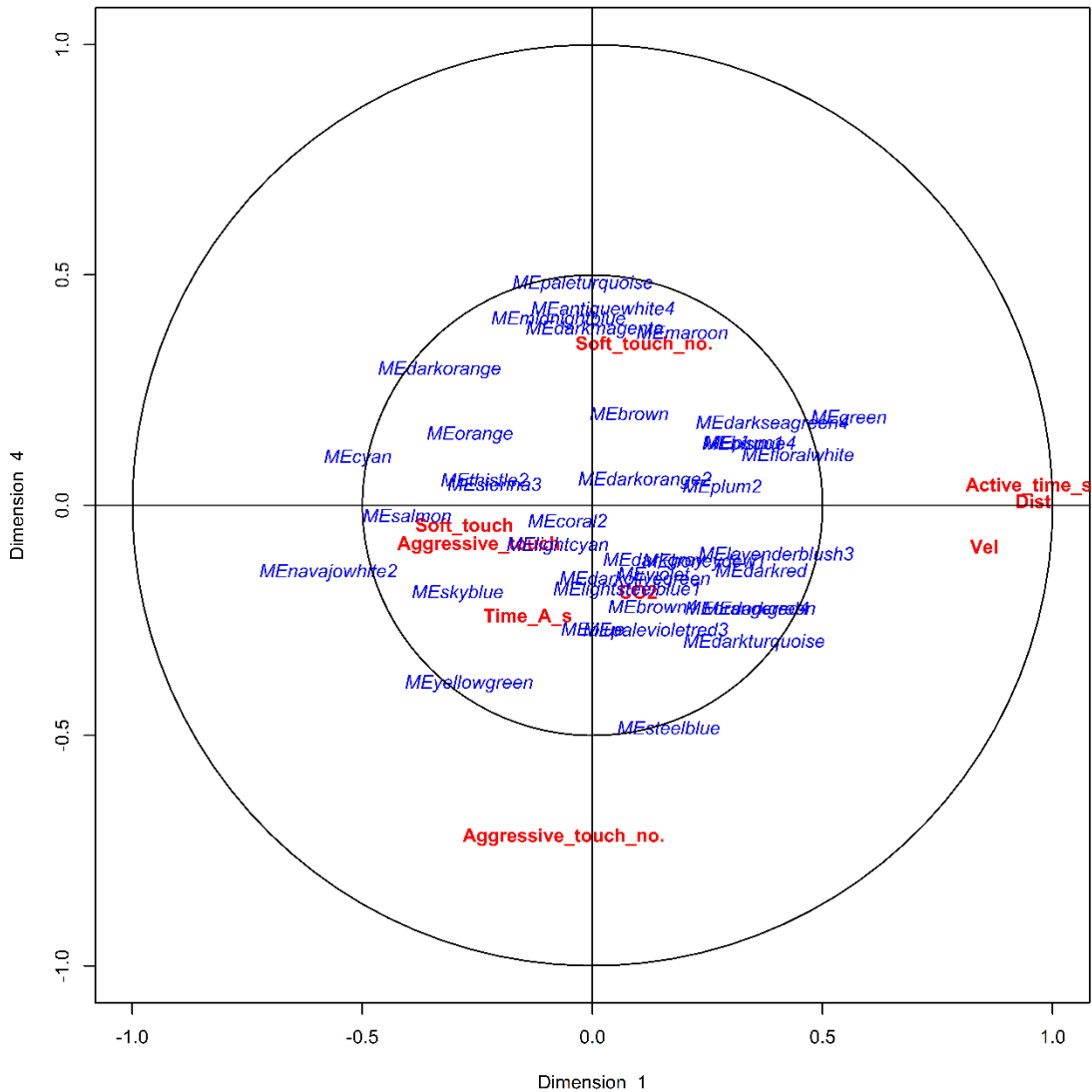
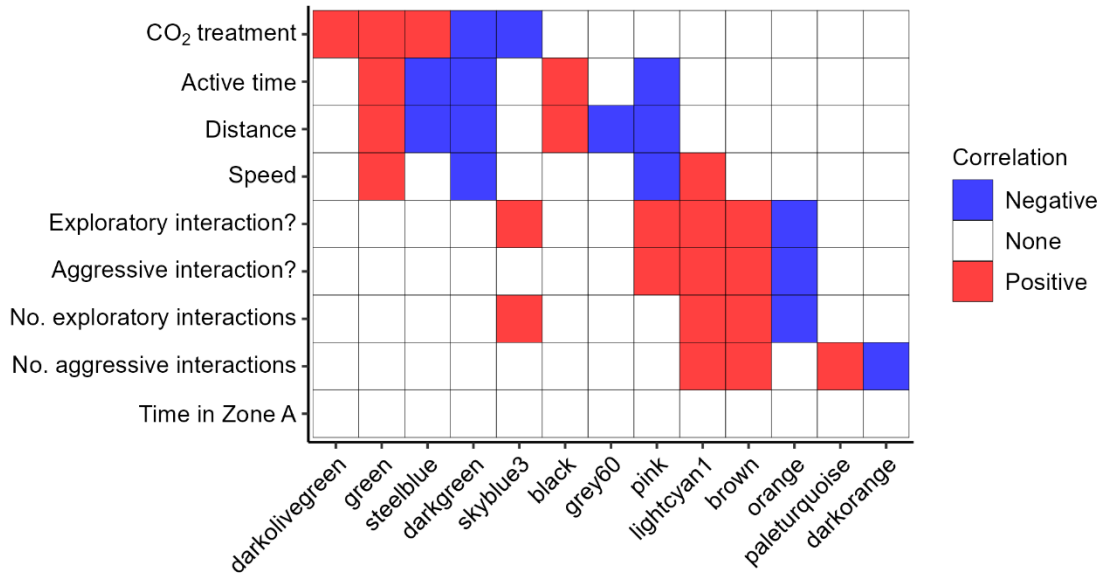


**Figure S18. Canonical correlation analysis biplot for the eyes canonical functions 1 and 4.** Depicting where the module eigengenes (MEs) lie in space in relation to the traits for the eyes, for canonical functions (dimensions) 1 and 4. Variables from the MEs set and the traits set are in blue and red, respectively. The inner ring is set at a radius of 0.5.





**A**



**B**

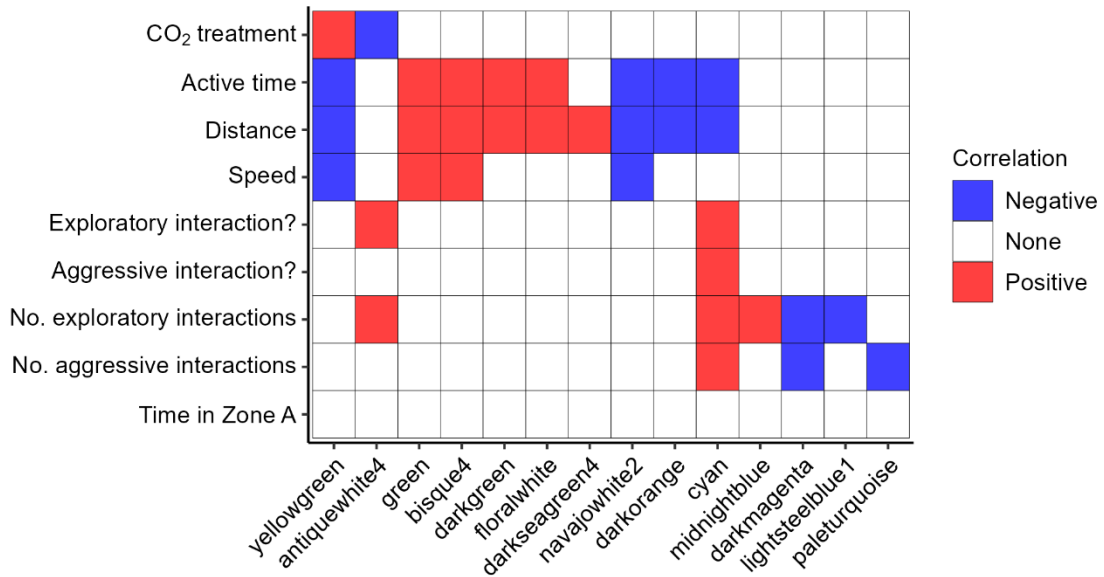


**Figure S21. Final modules of interest in the A) CNS and B) eyes.** Red = positive correlation between the trait and module eigengene, blue = negative correlation between the trait and module eigengene.

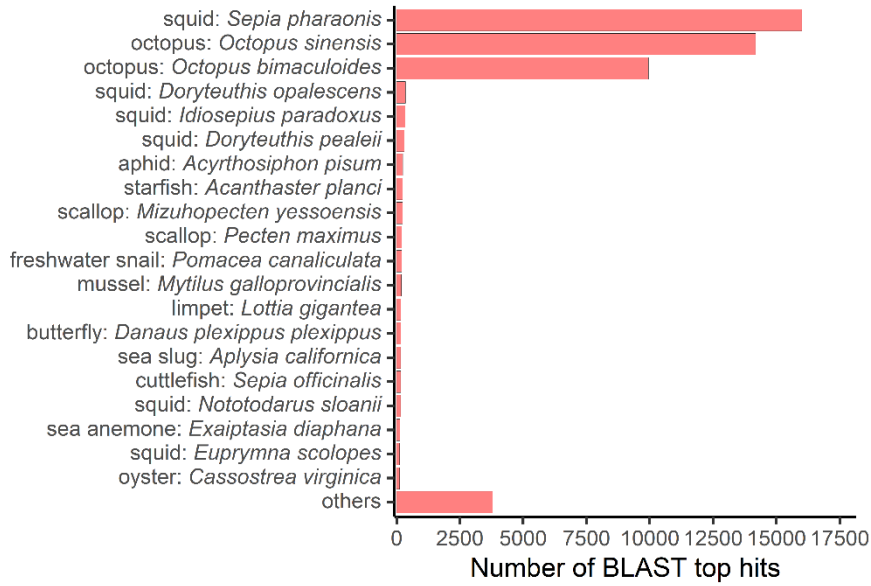


**Figure S22. Species distribution for the top blast hits of the annotated transcriptome assembly.** The top 29 species are shown. Others = the remaining 936 species grouped together.

See separate file for figure.

**Figure S23. Dotplot showing the results from gene set enrichment analysis (GSEA) using GO terms/functional categories in the CNS and eyes.** CNS = central nervous system, padj = adjusted p-value, count = number of core enrichment genes in the GO term/functional category.

## Supplementary Tables

See separate excel file for tables

**Table S1. Table of 27 modules detected in the CNS, with the number of genes within each module.**

**Table S2. Table of 38 modules detected in the eyes, with the number of genes within each module.**

**Table S3. Quality and completeness measures of the transcriptome assembly.** The PacBio Sequel II produced a total of 138.6 million subreads which were used to assemble the de novo transcriptome. Before redundancy removal = ISO-seq data processed with the isoseq3 pipeline. After redundancy removal = ISO-seq data processed with the isoseq3 pipeline followed by redundancy removal with CD-HIT-EST. Final transcriptome assembly = ISO-seq data processed with the isoseq3 pipeline, followed by redundancy removal with CD-HIT-EST and only the transcripts containing an ORF, as identified by TransDecoder, were retained. bp = base pairs.

**Table S4. Annotation measures of the transcriptome assembly.**

**Table S5. RNA-sequencing information for each sample.** CNS = central nervous system, eyes = both eyes combined from the same individual, % mapping rate is mapping of the trimmed and decontaminated RNA-seq reads against the final transcriptome assembly.

**Table S6. Table of DEGs and their putative function in the CNS and eyes, ordered by LFC.** Genes in red and blue are upregulated and downregulated at elevated CO<sub>2</sub>, respectively. DEGs in both tissues are in bold. padj = adjusted p-value, LFC = log<sub>2</sub> fold change.

**Table S7. Eyes-specific CO<sub>2</sub> treatment hub genes.** For each of these CO<sub>2</sub> treatment hub genes, those genes also identified as a hub gene for one or more behavioural traits in the eyes are indicated in the columns on the right (active time, distance, speed, no. exploratory interactions). The numbers in each column are the gene significance (GS) for the corresponding trait (-1 to 1). Positive GS = positive correlation between gene expression and trait (in red), negative GS = negative correlation between gene expression and trait (in blue). The larger the GS absolute value the more biologically relevant the gene is. Dist. = distance, No. EI = number of exploratory interactions.

**Table S8. Hub genes identified for CO<sub>2</sub> treatment in both the CNS and eyes.** For each of these CO<sub>2</sub> treatment hub genes, those genes also identified as a hub gene for a behavioural trait in the CNS or eyes are indicated in the columns on the right (active time, distance, speed, no. exploratory interactions). The numbers in each column are the gene significance (GS) for the corresponding trait (-1 to 1). Positive GS = positive correlation between gene expression and trait (in red), negative GS = negative correlation between gene expression and trait (in blue). The

larger the GS absolute value the more biologically relevant the gene is. Dist. = distance, No. EI = number of exploratory interactions.

**Table S9. CNS-specific CO<sub>2</sub> treatment hub genes.** For each of these CO<sub>2</sub> treatment hub genes, those genes also identified as a hub gene for one or more behavioural traits in the CNS are indicated in the columns on the right (active time, distance, speed, no. exploratory interactions, exploratory interaction?). The numbers in each column are the gene significance (GS) for the corresponding trait (-1 to 1). Positive GS = positive correlation between gene expression and trait (in red), negative GS = negative correlation between gene expression and trait (in blue). The larger the GS absolute value the more biologically relevant the gene is. Dist. = distance, No. EI = number of exploratory interactions, Exploratory interaction? = whether any exploratory interactions occurred (yes/no).

**Table S10. List of function groups and related CNS-specific hub genes shared by CO<sub>2</sub> treatment and one or more activity traits.**

**Table S11. All core enrichment genes from the cluster of GO terms/functional categories related to ligand-gated ion channels that were found significant with gene set enrichment analysis in both the CNS and eyes.** The ion channel cluster includes the GO terms 'ionotropic glutamate receptor signaling pathway', 'ionotropic glutamate receptor activity', 'postsynaptic membrane', 'excitatory postsynaptic potential', 'ion transmembrane transport', 'acetylcholine-gated cation-selective channel activity', 'transmembrane signaling receptor activity', 'extracellular ligand-gated ion channel activity', 'synapse', and 'ion channel activity'. Gene = gene ID in the transcriptome, annotation = annotation of the corresponding gene, ordered alphabetically.

**Table S12. All core enrichment genes from the cluster of GO terms/functional categories related to GPCR (G-protein coupled receptors) that were found significant with gene set enrichment analysis in the CNS (no GPCR GO terms found significant in the eyes).** The GPCR cluster includes the GO terms 'G protein-coupled receptor activity' and 'G protein-coupled receptor signaling pathway'. Gene = gene ID in the transcriptome, annotation = annotation of the corresponding gene, ordered alphabetically.

**Table S13. All core enrichment genes from the cluster of GO terms/functional categories related to ion transport that were found significant with gene set enrichment analysis in the CNS (no ion transport GO terms found significant in the eyes).** The ion transport cluster includes the GO terms 'potassium channel activity', 'potassium ion transmembrane transport', 'voltage-gated potassium channel activity', 'regulation of ion transmembrane transport', 'voltage-gated calcium channel complex', and 'calcium ion transmembrane transport'. Gene = gene ID in the transcriptome, annotation = annotation of the corresponding gene, ordered alphabetically.

**File S1. TapeStation electropherograms for each of the 40 RNA samples used for RNA-sequencing.** Each sample is labelled by its individual ID and the tissue type. RNA integrity of all 40 samples was measured on an Agilent 2200 TapeStation (High Sensitivity RNA ScreenTape, Agilent), without the sample denaturation step due to denaturation removing the 28S peak, likely due to a 'hidden break' as reported in some other animals (Winnebeck *et al.*, 2010). All central nervous system (CNS) RNA had an equivalent RNA integrity (RINe)  $\geq 8.5$  (mean 9.3, SD 0.3). For the eye samples, a RINe value could not be obtained due to the TapeStation being unable to detect the lower marker, likely due to carry over of pigment into the eye RNA samples. A Femto Pulse system (Ultra Sensitivity RNA Kit, Agilent) did obtain RNA Quality Scores (RQN): eye RQN  $\geq 4.8$  (mean 6.5, SD 1.3). The four samples also used for ISO-sequencing are outlined in thick black. CNS samples used for ISO-seq had RINe values of 9.4 and 9.5. Before ISO-seq, RNA from the eyes was purified with oligo d(T) beads due to carry over of pigmentation (NEBNext<sup>®</sup> Poly(A) mRNA Magnetic Isolation Module, New England BioLabs Inc.), followed by integrity assessment on a Femto Pulse system (Ultra Sensitivity RNA Kit, Agilent). After purification, eyes samples had an RQN of 6.1 and 8.6.

See separate file.

## References

- BioBam Bioinformatics.** (2019). *OmicBox - Bioinformatics made easy (Version 1.4.12)*.  
<https://www.biobam.com/omicsbox>.
- Brian, H. and Papanicolaou, A.** (n.d.). *Transdecoder (Find Coding Regions Within Transcripts)*.  
<http://transdecoder.github.io>.
- Camacho, C., Coulouris, G., Avagyan, V., Ma, N., Papadopoulos, J., Bealer, K. and Madden, T. L.** (2009). BLAST+: Architecture and applications. *BMC Bioinformatics* **10**, 1-9.
- Dickson, A. and Millero, F. J.** (1987). A comparison of the equilibrium constants for the dissociation of carbonic acid in seawater media. *Deep Sea Research Part A. Oceanographic Research Papers* **34**, 1733-1743.
- Dickson, A. G., Sabine, C. L. and Christian, J. R.** (2007). *Guide to Best Practices for Ocean CO<sub>2</sub> Measurements. PICES Special Publication 3*. Sidney, Canada: North Pacific Marine Science Organization.
- Evans, J. D.** (1996). *Straightforward Statistics for the Behavioral Sciences*: Thomson Brooks/Cole Publishing Co.
- Fu, L., Niu, B., Zhu, Z., Wu, S. and Li, W.** (2012). CD-HIT: Accelerated for clustering the next-generation sequencing data. *Bioinformatics* **28**, 3150-3152.
- Fuller, T. F., Ghazalpour, A., Aten, J. E., Drake, T. A., Lusic, A. J. and Horvath, S.** (2007). Weighted gene coexpression network analysis strategies applied to mouse weight. *Mammalian Genome* **18**, 463-472.
- González, I., Déjean, S., Martin, P. and Baccini, A.** (2008). CCA: An R package to extend canonical correlation analysis. *Journal of Statistical Software* **23**, 1-14.
- Götz, S., García-Gómez, J. M., Terol, J., Williams, T. D., Nagaraj, S. H., Nueda, M. J., Robles, M., Talón, M., Dopazo, J. and Conesa, A.** (2008). High-throughput functional annotation and data mining with the Blast2GO suite. *Nucleic Acids Research* **36**, 3420-3435.
- Hannan, K. D., Miller, G. M., Watson, S.-A., Rummer, J. L., Fabricius, K. and Munday, P. L.** (2020). Diel pCO<sub>2</sub> variation among coral reefs and microhabitats at Lizard Island, Great Barrier Reef. *Coral Reefs* **39**, 1391-1406.
- Horvath, S. and Dong, J.** (2008). Geometric interpretation of gene coexpression network analysis. *PLoS Computational Biology* **4**, e1000117-e1000117.
- Jones, P., Binns, D., Chang, H.-Y., Fraser, M., Li, W., McAnulla, C., McWilliam, H., Maslen, J., Mitchell, A., Nuka, G. et al.** (2014). InterProScan 5: Genome-scale protein function classification. *Bioinformatics* **30**, 1236-1240.
- Kabir, A., Merrill, R. D., Shamim, A. A., Klemm, R. D., Labrique, A. B., Christian, P., West Jr, K. P. and Nasser, M.** (2014). Canonical correlation analysis of infant's size at birth and maternal factors: a study in rural Northwest Bangladesh. *PLoS One* **9**, e94243.
- Lambert, Z. V. and Durand, R. M.** (1975). Some precautions in using canonical analysis. *Journal of Marketing Research* **12**, 468-475.
- Langfelder, P. and Horvath, S.** (2008). WGCNA: An R package for weighted correlation network analysis. *BMC Bioinformatics* **9**, 1-13.
- Langmead, B. and Salzberg, S. L.** (2012). Fast gapped-read alignment with Bowtie 2. *Nature Methods* **9**, 357-359.

- Li, W. and Godzik, A.** (2006). Cd-hit: A fast program for clustering and comparing large sets of protein or nucleotide sequences. *Bioinformatics* **22**, 1658-1659.
- Love, M. I., Huber, W. and Anders, S.** (2014). Moderated estimation of fold change and dispersion for RNA-seq data with DESeq2. *Genome Biology* **15**, 550.
- Manni, M., Berkeley, M. R., Seppely, M., Simão, F. A. and Zdobnov, E. M.** (2021). BUSCO update: Novel and streamlined workflows along with broader and deeper phylogenetic coverage for scoring of eukaryotic, prokaryotic, and viral genomes. *Molecular Biology and Evolution* **38**, 4647-4654.
- Mehrbach, C., Culberson, C., Hawley, J. and Pytkowicz, R.** (1973). Measurement of the apparent dissociation constants of carbonic acid in seawater at atmospheric pressure 1. *Limnology and Oceanography* **18**, 897-907.
- Sherry, A. and Henson, R. K.** (2005). Conducting and interpreting canonical correlation analysis in personality research: A user-friendly primer. *Journal of personality assessment* **84**, 37-48.
- Smith-Unna, R., Bournnell, C., Patro, R., Hibberd, J. M. and Kelly, S.** (2016). TransRate: Reference-free quality assessment of *de novo* transcriptome assemblies. *Genome Research* **26**, 1134-1144.
- Winnebeck, E. C., Millar, C. D. and Warman, G. R.** (2010). Why does insect RNA look degraded? *Journal of Insect Science* **10**, 159.